Topics on Modelling and Simulation of Wireless Networking Protocols

A Thesis

Submitted to the Faculty

of

Drexel University

by

Jeffrey W. Wildman II

in partial fulfillment of the

requirements for the degree

of

Master of Science in Electrical and Computer Engineering

April 2009

Dedications

To my grandmother, Joycelyn S. Wildman

Acknowledgements

Many thanks to:

Dr. Moshe Kam and Dr. Steven Weber, my advisors, for all of their guidance and advice

Dr. Siamak Dastangoo, for the opportunity to learn and work at MIT Lincoln Lab,

Dr. Glenn Carl, for his emulation testbed work and constructive criticism,

past and current labmates at the Data Fusion Lab and ACIN,

my friends for putting up with my frequent aloofness,

my family for the two-day getaways called weekends,

and

Becky, for her patience, love, and support.

Table of Contents

List of Figures

List of Tables

List of Acronyms

AA Addressing Agent.

ACK Acknowledgement.

AODV Ad hoc On-Demand Distance Vector.

ATM Asynchronous Transfer Mode.

BDR Backup Designated Router.

BER Bit Error Rate.

BIDIR Bi-directional.

BMDR Backup MANET Designated Router.

CTS Clear to Send.

DAD Duplicate Address Detection.

DbDesc Database Description.

DCF Distributed Coordination Function.

DES Discrete Event Simulator.

DPSK Differential Phase Shift Keying.

DR Designated Router.

DSDV Destination-Sequenced Distance Vector.

DSSS Direct-Sequence Spread Spectrum.

ETE End-to-End.

FTP File Transfer Protocol.

GW_INFO Gateway Information.

HCQA Hybrid Centralized Query-based Autoconfiguration.

IEEE Institute of Electrical and Electronics Engineers.

IETF	Internet Engineering Task Force.
IP	Internet Protocol.
IPv6	Internet Protocol version 6.
J&N	Jelger & Noel.
LSA	Link State Advertisement.
LSAck	Link State Acknowledgement.
LSReq	Link State Request.
LSU	Link State Update.
MAC	Medium Access Control.
MANET	Mobile Ad hoc Network.
MDR	MANET Designated Router.
MPR	Multipoint Relay.
NAV	Network Allocation Vector.
NBMA	Non-Broadcast Multiple Access.
OLSR	Optimized Link State Routing.
OR	Overlapping Relays.
OSPF	Open Shortest Path First.
OSPFv3	Open Shortest Path First version 3.
PACMAN	Passive AutoConfiguration for Mobile Ad hoc Networks.
PDAD	Passive DAD.
PTMP	Point-to-Multipoint.
PTP	Point-to-Point.
QDAD	Query-based DAD.

R-OSPF Radio-OSPF.

RFC Request for Comments.

RTS Request to Send.

RTS/CTS Request to Send/Clear to Send.

RWP Random Waypoint.

SI-CDS Source Independent Connected Dominating Set.

SINR Signal to Interference and Noise Ratio.

UDP User Datagram Protocol.

VLAN Virtual Local Area Network.

WDAD Weak DAD.

WLAN Wireless Local Area Network.

Abstract

Topics on Modelling and Simulation of Wireless Networking Protocols

Jeffrey W. Wildman II
Advisors:
Steven Weber, Ph.D.
Moshe Kam, Ph.D., P.E.

The use of computer simulation to study complex systems has grown significantly over the past several decades. This is especially true with regard to computer networks, where simulation has become a widespread tool used in academic, commercial and military applications. Computer model representations of communication protocol stacks are used to replicate and predict the behavior of real world counterparts to solve a variety of problems.

The performance of simulators, measured in both accuracy of results and run time, is a constant concern to simulation users. The running time for high fidelity simulation of large-scale mobile ad hoc networks can be prohibitively high. The execution time of propagation effects calculations for a single transmission alone can grow unmanageable to account for all potential receivers. Discrete event simulators can also suffer from excessive generation and processing of events, both due to network size and model complexity. In this thesis, three levels of abstracting the Institute of Electrical and Electronics Engineers (IEEE) 802.11 Request to Send/Clear to Send (RTS/CTS) channel access mechanism are presented. In the process of assessing the abstractions' ability to mitigate runtime-cost while retaining comparable results to that of a commercially available simulator, OPNET, the abstractions were found to be better suited to collecting one metric over another.

Performance issues aside, simulation is an ideal choice for use in prototyping and developing protocols. The costs of simulation are orders of magnitude smaller than that of network testbeds, especially after factoring in the logistics, maintenance, and space required to test live networks. For instance, Internet Protocol version 6 (IPv6) stateless address autoconfiguration protocols have yet to be convincingly shown to cope with the dynamic, infrastructure-free environment of Mobile Ad hoc Networks (MANETs). This thesis provides a literature survey of autoconfiguration schemes designed for MANETs, with particular focus on a stateless autoconfiguration scheme by Jelger and

Noel (SECON 2005). The selected scheme provides globally routable IPv6 prefixes to a MANET attached to the Internet via gateways. Using OPNET simulation, the Jelger-Noel scheme is examined with new cluster mobility models, added gateway mobility, and varied network sizes. Performance of the Jelger-Noel scheme, derived from overhead, autoconfiguration time and prefix stability metrics, was found to be highly dependent on network density, and suggested further refinement before deployment.

Finally, in cases where a network testbed is used to test protocols, it is still advantageous to run simulations in parallel. While testbeds can help expose design flaws due to code or hardware differences, discrete event simulation environments can offer extensive debugging capabilities and event control. The two tools provide independent methods of validating the performance of protocols, as well as providing useful feedback on correct protocol implementation and configuration. This thesis presents the Open Shortest Path First (OSPF) routing protocol and its MANET extensions as candidate protocols to test in simulated and emulated MANETs. The measured OSPF overhead from both environments was used as a benchmark to construct equivalent MANET representations and protocol configuration, made particularly challenging due to the wired nature of the emulation testbed. While attempting to duplicate and validate results of a previous OSPF study, limitations of the simulated implementation of OSPF were revealed.

1. Introduction

The use of computer simulation to study complex systems has grown significantly over the past several decades. This is especially true with regard to computer networks, where simulation has become a widespread tool used in academic, commercial and military applications. Computer model representations of communication protocol stacks are used to replicate and predict the behavior of real world counterparts to solve a variety of problems.

The popularity of simulation stems from the fact that computing power continually becomes faster and cheaper. The cost of simulation hardware and software has become orders of magnitude smaller than that of network testbeds, especially for large networks. Simulation also avoids the logistics, maintenance, and space required to test live networks, such as mobile ad hoc networks with complex, coordinated movement patterns [1]. Often, simulation is used to answer queries about the performance of a network *prior* to making investments in hardware and bandwidth. Simulations can advise on the minimal set of hardware required to provide a desired quality of service; examples include expanding commercial networks to support additional offices, overprovisioning by Internet Service Providers, and determining buffer sizes for streaming media over the Internet.

Several features of computer simulation prove to be extremely beneficial for research and development of new and existing network protocols. Discrete event simulation environments can offer extensive debugging capabilities and event control, such as the ability of stopping time and stepping through events to examine the states and interaction of model internals. Reproducible simulation runs, controlled by a random seed, allow the re-creation of particular events of interest in protocol operation. Students can also take advantage of all of these characteristics of simulation in the classroom to learn more about computer networking.

However, the performance of simulations, both in accuracy of results and run time, are a constant concern of the users of such software. Simulators are not bound to a 1:1 ‘real-time’ run time, which can result in wildly varying speedup or slowdown factors. The run time is largely dependent on the fidelity of the models and the number of devices being simulated [2]. In cases where estimates of network performance are time-critical, such as military deployments or natural disaster responses, the simulated networks are likely to be very large and the simulation results must be extremely accurate. Additionally, simulation of a network may not provide certain vital information about the ‘production model’. Differences in protocol stack implementation and hardware may hide software bugs from view until testbeds are employed [1, 3].

The combined benefits and drawbacks of computer network simulation provide a large variety of research problems to the research community, both to employ simulation to solve problems and to resolve problems with the simulation process itself. This thesis is comprised of three case studies that *a)* highlight issues affecting the use of simulation, as well as *b)* detail ways of applying simulation to the study of wireless networking protocols.

Chapter 2 examines the tradeoff between running time and model fidelity for large-scale Mobile Ad hoc Network (MANET) simulations. Three levels of abstracting the Institute of Electrical and Electronics Engineers (IEEE) 802.11 Request to Send/Clear to Send (RTS/CTS) channel access mechanism are presented and simulated against a commercially available network simulator, OPNET. The abstractions are assessed by their ability to mitigate runtime cost while retaining comparable results to the commercial simulator. The abstractions are found to be better suited to collecting some metrics than others. This work was presented at MILCOM 2006 [4].

Chapter 3 examines the feasibility of a new protocol via simulation. A literature survey of autoconfiguration schemes designed for MANETs is provided, with particular focus on a stateless autoconfiguration scheme by Jelger and Noel (SECON 2005) [5]. The selected scheme provides globally routable Internet Protocol version 6 (IPv6) prefixes to a MANET attached to the Internet via gateways. Using OPNET simulation, the Jelger-Noel scheme is examined with new cluster mobility models, gateway mobility, and varied network sizes. Performance of the Jelger-Noel scheme, measured from overhead, autoconfiguration time and prefix stability metrics, is found to be highly dependent on network density, and suggests further refinement before deployment. This work was presented at MILCOM 2007 [6].

In Chapter 4, simulations are used to cross-validate an emulation testbed running the Open Shortest Path First (OSPF) routing protocol and its MANET Designated Router (MDR) extension. The measured OSPF overhead from both environments is used as a benchmark to construct equivalent MANET representations and protocol configuration, made particularly challenging due to the wired nature of the emulation testbed. Compromises are struck between the emulation and simulation environments to bring routing overhead and packet rate measurements within acceptable levels between the environments. While attempting to duplicate and validate results of a previous OSPF study, limitations of the simulated implementation of OSPF are revealed. Specifics on the emulation testbed configuration were presented at MILCOM 2008 [7].

Finally, Chapter 5 summarizes each of the three studies and highlights important findings.

2. RTS-CTS Abstractions

2.1 Introduction

Meaningful simulation of ad hoc wireless networks is a time-intensive task and reducing the execution time is important, particularly when planning networks for use in military operations. For such simulations, the desired scale can range from hundreds to thousands of radios and the results are often needed within hours or days. For large ad hoc networks, the most computation-intensive tasks in simulation are computing interference and determining which receivers are in range of a transmitter. In both cases, $O(N^2)$ physical layer calculations are required for a wireless system of N nodes, which scales poorly.

There are several proposals to improve the running time necessary to calculate the inter-nodal interference. Naoumov and Gross [8] introduce a 3-dimensional array of pointers to nodes ordered by x- and y-coordinates, which they use to reduce the amount of space searched for nodes within range of the transmitter. A similar approach is employed in this study but, while [8] focuses on reducing the number of potential interferers, we focus instead on reducing the number of calculations necessary to determine the set of potential receivers. Several techniques, or abstractions, are presented to improve scalability and decrease running time of an Institute of Electrical and Electronics Engineers (IEEE) 802.11 wireless model while achieving equivalent simulation results to that of a commercially available simulator, OPNET. In the process of assessing the abstractions' ability to mitigate runtime cost, the abstractions were found to be better suited to collecting some metrics over others.

The rest of this chapter is organized as follows. Section 2.2 contains a survey of related research. Section 2.3 presents models and the parameters of the custom-built simulator running abstractions of the IEEE 802.11 protocol. Section 2.4 describes the proposed abstraction models. Section 2.5 introduces the validation method used and highlights the differences between the custom simulator and OPNET Modeler [9]. In Section 2.6, results gathered from both simulators are compared and discussed. Section 2.7 concludes the chapter and suggests possible avenues of future work on this topic.

2.2 Survey of Literature on Simulation Performance

Previous studies of mobile network simulation suggest two primary methods for improving simulation performance: parallel programming (assuming multiple processors are available) [10–12] and model abstraction [1,13]. Each of these methods involves certain trade-offs. A parallelized approach may scale well without losing accuracy but at a high cost in computing resources, while abstraction improves execution time but may sacrifice some degree of accuracy. Additionally, these methods are not mutually exclusive and may be employed together.

The physics of radio transmission introduce challenges to simulation not present with wired networks [14]. The one-to-many broadcast nature of wireless transmissions is fundamentally different than one-to-one communication in wired networks. In a radio-connected network, the distances at which a transmission can be successfully received and at which a transmission may cause interference may be different [8]. Takai, et al. [15] provide a good description of several approaches to modeling the physical layer and the consequences of choosing one model over another. A simulation is a simplification of a real-world system [16] and careful consideration must be given to the details omitted. A good summary of the issues involved is given by Heidemann, et al. [14]. Cavin, et al. [17] discuss issues relating to the accuracy of mobile ad hoc network simulators and ways of analyzing the results.

A highly detailed network model often greatly reduces scalability, meaning the model is infeasible for simulating large networks. However, less detailed models can reduce the reliability of the results. Blum, et al. [2] introduce a 'dual mode' approach that dynamically switches between detailed simulation models and abstractions depending on network conditions. Naoumov and Gross [8] reduce execution time by exploiting the probability that nodes will be spread throughout the modeled space. Perrone and Nicol [18] use the Barnes-Hut (N-body) algorithm based on the observation that the gravitational pull between objects in astrophysical models is similar to signal attenuation models of wireless models in that both decay polynomially with distance. The amount of detail that can safely be abstracted out depends on what network behavior is being studied, as discussed by Liu, et al. [19] and by Zhong and Rabaey [20]. Golmie, et al. [21] and Heindl and German [22] present approaches to modeling the IEEE 802.11 protocol.

2.3 Custom-built Simulator Models

A packet-based, Discrete Event Simulator (DES) was developed for the purposes of this study. The simulator includes models at the physical, medium access, and application layers in addition to mobility models. Nodes are all modeled homogeneously and are described by their mobility, traffic generation, and transmission protocol.

2.3.1 Mobility

A Random Waypoint (RWP) [23] model captures the network's dynamic topology. Initial node positions are chosen independently and uniformly at random from the entire 1 km by 1 km simulation space. Nodes travel at a constant speed of 1 m/s, and choose destinations (waypoints) uniformly from the arena without a 'pause time' between waypoints. This movement model was selected both for simplicity and to avoid the transient behavior inherent in certain RWP models in which nodes experience a 'slowdown' over time [24].

2.3.2 Traffic

The application layer consists of a basic source and sink. Nodes generate packets for the duration of the simulation. Each node's packet generation times form an independent and identically distributed Poisson point process. Packet sizes are chosen from an exponential distribution with a mean of 128 bytes. The destination of each packet is picked uniformly from the full set of nodes.

2.3.3 Transmission

At the physical layer, the Friis transmission equation governs signal attenuation:

$$P_r^{i,j}(t) = \frac{P_t^i(t)\, G_t\, G_r\, \lambda^2}{(4\pi)^2\, d_{i,j}^{\alpha}(t)} \ \text{(mW)} \tag{2.1}$$

where $P_r^{i,j}(t)$ is the received power at node j from transmitting node i at time t, $P_t^i(t)$ is the transmitted power at node i, and $d_{i,j}(t)$ is the distance between transmitter i and receiver j (in meters). Transmitter and receiver antenna gains, G_t and G_r, are assumed to be isotropic and are set to 2. The wavelength λ (in meters) is derived from the first IEEE 802.11b Direct-Sequence Spread Spectrum (DSSS) channel's center-frequency of 2.412 GHz. The pathloss constant α is set to 4 to model stronger signal attenuation than free space [25].

Interference power measured at node j at time t, given a desired transmission from node i, is given by:

$$I_j(t) = \sum_{k \in \mathcal{T}(t) \setminus i} P_r^{k,j}(t) \ \text{(mW)} \tag{2.2}$$

where $\mathcal{T}(t)$ is the set of all transmitting nodes at time t.

A Bit Error Rate (BER) model is used in addition to (2.1) and (2.2) to evaluate a signal's likelihood for success. It maps received power and interference levels to a BER assuming a Differential Phase Shift Keying (DPSK) modulation scheme:

$$\text{BER} = 0.5 \exp\left(\frac{-E_b}{N_o + I/R}\right). \tag{2.3}$$

Here, R is the data rate, E_b is the received energy per bit (P_r/R), I/R is the interference energy per bit, and N_o accounts for noise from the environment and the receiver's electronics. N_o is derived from an achievable BER at a given receiver sensitivity and data rate. At 11 Mbps, nodes were assumed to experience a BER of 10^{-4} at a receiver sensitivity of $P_r = -95$ dBm. These parameters assume zero interference ($I = 0$ mW) which allows (2.3) to be rearranged to solve for $N_o = 3.38 \times 10^{-18}$ mW. Use of (2.3) during simulation is then carried out for a calculated received power P_r, aggregate interference power I, and the pre-solved N_o.

Transmission success is determined by modeling the number of bit errors n_{error} incurred during packet transmission as a binomial random variable $n_{\text{error}} \sim B(n, p)$ with n total bits and a BER of p. Since error correction is not modeled, a single error will result in a dropped packet. The probability of packet success equates to generating $n_{\text{error}} = 0$ bit errors and assuming each bit in a packet is in error independently, the packet success rate is $(1 - p)^n$.

The simulator maintains a network-wide list of transmitting packets. The list is updated dynamically as packets start and finish transmitting. Whenever a packet is added, the BER is recalculated for every packet on the list to reflect new interference conditions. Each packet's new BER is then used to predict the number of errors over the entire length of the packet. If any errors are predicted, the transmission attempt corresponding to the packet is marked as failed. Once a packet is marked as failed, it remains as such. Figure 2.1 shows a sample trace of packet transmissions that begin at times $t1$, $t2$, and $t4$. Over the course of the sample packet timing chart, physical layer calculations are performed at times $t1$ and $t2$ for packet 1, times $t2$, $t3$, and $t4$ for packet 2, and times $t4$ and $t5$ for packet 3. Additionally, transmission times do not include propagation delay.

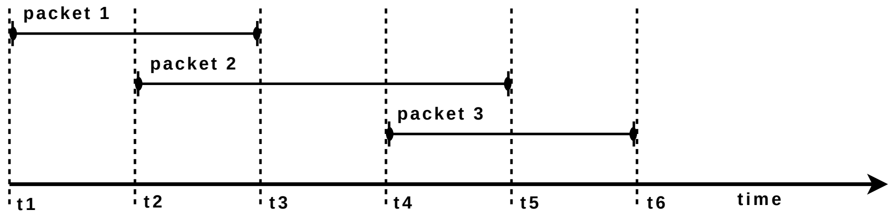

Figure 2.1: Example timing chart of packet transmissions.

2.4 IEEE 802.11 Model Abstractions

The custom-built simulator's medium access layer contains three abstractions of the IEEE 802.11 Standard. Sources used in implementation include [25] and [26]. Given the infrastructureless nature of ad hoc networks, all abstractions use the Distributed Coordination Function (DCF) to handle media access control. A Network Allocation Vector (NAV) is used in conjunction with binary exponential back-off to determine medium access. Physical carrier sensing (via beaconing) is not simulated, but virtual carrier sensing is accomplished by the Request to Send/Clear to Send (RTS/CTS) mechanism. Every packet initiates an RTS/CTS sequence, regardless of its size. Packets are not fragmented, and large packets are dropped immediately upon reaching the datalink layer. Packets' sizes are increased by 292 bytes at the medium access layer to account for headers and physical layer overhead (to match OPNET), which results in an overall mean packet size of $128 + 292$ bytes. Packet queues are maintained at each node with a maximum size of 32 KB of simulated data, and packets are dropped after four transmission attempts. The exact implementation of RTS/CTS for each model differs, as each model adds an additional degree of abstraction to the previous one. Note that nodes use only one of the abstractions during any given simulation to maintain homogeneity. The remainder of this section discusses the three developed abstractions, the Event-Compression, Neighbor List, and Simplified Neighbor List models.

2.4.1 Event-Compression Model

Of the three abstractions to be presented, the Event-Compression model strays the least from the validation model (discussed in Section 2.5) in terms of implementation. Specifically, its most significant abstractions are the use of a collapsed-RTS/CTS and implicit acknowledgement. Both

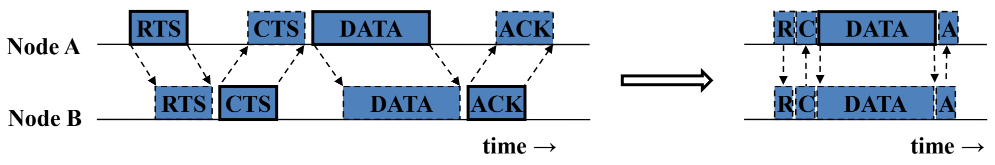

Figure 2.2: The RTS/CTS handshaking procedure (left) between nodes A and B is abstracted (right) to that the individual (R)TS and (C)TS control packets are transmitted instantaneously and the (A)CK control packet is treated as an implicit notification between the pair of nodes. Only the DATA packet is modelled in full.

assume that the DATA packet's size, large relative to the size of the control packets, will take the bulk of transmission time from transmitter to receiver. The Request to Send (RTS) and Clear to Send (CTS) control packets are transmitted instantaneously and are not modeled by separate events, but are still subjected to BER calculations to determine success or failure. The Acknowledgement (ACK) packet is also abstracted away by implicitly 'notifying' the transmitter of the DATA packet's reception (without BER calculations). Control packet 'transmissions' do not produce interference for DATA packets. A DES maintains a temporally-ordered list of events, and the running time of the DES is affected by the number of events to be processed. The abstractions present in this model recognize the link between the number of events in a simulation and a DES's running time: they seek to reduce the number of events generated and processed during simulation.

Under this model, the RTS/CTS algorithm begins when a node's NAV indicates that the medium is free. The node takes the next DATA packet from the buffer and then calculates the reach of an RTS packet through physical layer calculations for every potential receiver, and updates the NAV of these nodes (potential receivers must also be idle). If the DATA packet's destination is included in this set of nodes, then the reach of the CTS (using the DATA packet's destination as the source) is calculated and NAVs are updated in the same manner. Finally, if the original source was included in the set of nodes that could hear the CTS, then the RTS/CTS is successful and the DATA packet is transmitted. The transmitter is notified of the DATA packet's status through the implicit ACK, and will retransmit if allowed. This process is visualized in Figure 2.2.

For one RTS or CTS packet, this procedure involves physical layer calculations for nearly every node (excluding the transmitter) in the network. In terms of Figure 2.3, the Event-Compression model evaluates the control packet's reception at every node within the entire simulation arena. While computationally costly, this should be the most accurate of the three models. For pseudocode, see the Event-Compression RTS/CTS procedure in Appendix Section A.1.

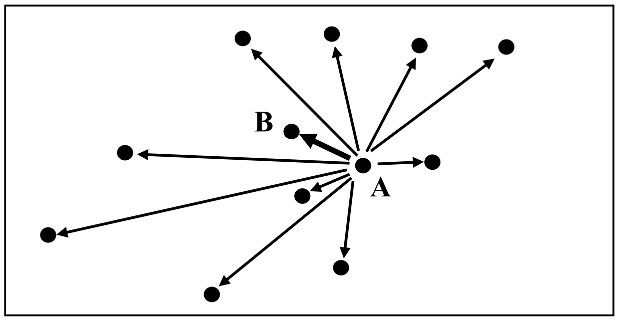

Figure 2.3: Using the Event Compression abstraction, the reception of a broadcasted control packet (from node A) is calculated at every potential receiver (along all arrows).

2.4.2 Neighbor List Model

While it is important to cut down on the number of events generated and processed during simulation, reducing the amount of computation per event is also crucial. The Neighbor List model is similar to the Event-Compression model, but modifies how the reach of control packets is calculated in an effort to reduce runtime. Each node maintains a list of 'reachable' neighbors that is updated periodically. Reachable nodes are those within the threshold distance required to successfully receive an interference-free transmission, where the 'neighbor distance' d_{max} is found by re-formulating (2.1):

$$d_{\text{max}} = \left(\frac{P_t\, G_t\, G_r\, \lambda^2}{P_r\, (4\pi)^2} \right)^{1/\alpha} \text{ (meters)}. \tag{2.4}$$

P_r assumes the value of the receiver sensitivity to produce the threshold distance for communication. The average number of neighbors then depends on the fraction of the area swept out by the neighbor distance to the entire area:

$$N \frac{\pi d_{\text{max}}^2}{A} \tag{2.5}$$

where N is the total number of nodes. Furthermore, the neighbor list update interval is specified as a function of node speed v:

$$t_{\text{int}} = \frac{\frac{1}{2} d_{\text{max}}}{v} \text{ (seconds)}. \tag{2.6}$$

Thus, t_{int} is the time a node takes to travel half the neighbor distance.

The neighbor list is used as the abridged list of potential receivers when calculating the reach of RTS and CTS packets. The motivation for this abstraction stems from two observations. One is that a neighbor list represents the best-case reach for a transmission and any attempt to broadcast a

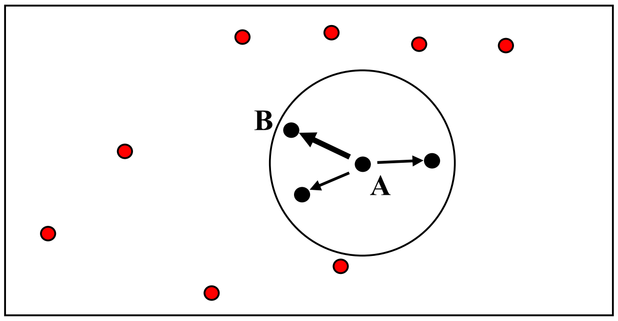

Figure 2.4: Using the Neighbor List abstraction, the reception of a broadcasted control packet (from node A) is calculated at every neighboring receiver (along all arrows). The broadcast is assumed to fail at all receivers outside of the neighbor distance (red nodes).

control packet would be successfully forwarded only to a subset of a properly updated neighbor list. Additionally, the topology of the network will remain effectively constant for appropriately chosen time intervals. Selecting t_{int} represents a tradeoff between the overhead of updating the neighbor list and keeping it accurate.

The benefits of this abstraction will vary according to the transmit power and speed assigned to nodes. P_t indirectly affects $d_{\max}$ through (2.4) and (2.5), and can cause the neighbor distance to encompass a significant portion of the simulation space. As the neighbor distance approaches the magnitude of the simulation space's dimensions, the Neighbor List abstraction's performance should approach that of the Event-Compression model. Similarly, as node mobility increases, the neighbor list will be updated at a more rapid pace (2.6), to the point that the extra time spent updating neighbor lists supercedes the time saved in the RTS/CTS reach calculations.

The method that calculates the neighbor list and the method to determine the neighbor list update rate are heuristics employed in an attempt to cut down computation. For one RTS or CTS packet, physical layer calculations are only needed for each neighbor, specified by (2.5). Instead of performing physical layer calculations on the entire network, only a subset of nodes is involved, which will reduce simulation runtime. Referring to Figure 2.4, the Neighbor List abstraction only evaluates the control packet's reception within the neighbor distance. The Neighbor List RTS/CTS procedure, located in Appendix Section A.2, illustrates this in pseudocode.

2.4.3 Simplified Neighbor List

The Simplified Neighbor List extends the Neighbor List abstraction by simplifying the transmission of control packets even further. A neighbor list is maintained in the same manner as described

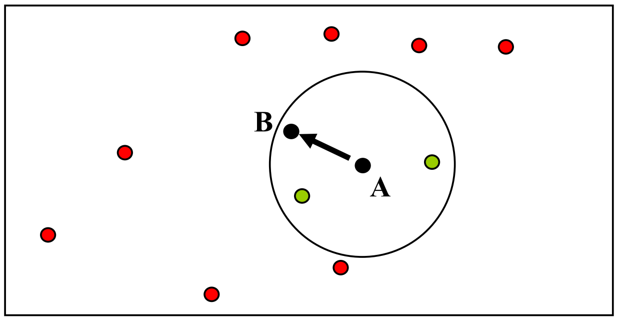

Figure 2.5: Using the Simplified Neighbor List abstraction, the reception of a broadcasted control packet (from node A) is calculated only at the target destination (node B). The broadcast is assumed to be successful at all nodes inside the circular neighbor region (green nodes). The broadcast is assumed to fail at all receivers outside of the neighbor distance (red nodes).

in Section 2.4.2. This model then calculates the RTS or CTS packet's reception only at the intended receiver and then assumes that all remaining potential receivers (i.e., remaining nodes in the neighbor list) successfully receive the packet. Looking at Figure 2.5, the Simplified Neighbor List abstraction evaluates control packet reception at the target destination RX only. All other nodes within the circular neighbor region automatically receive the control packet. The Simplified Neighbor List RTS/CTS procedure is explained in pseudocode in Appendix Section A.3.

For one RTS or CTS packet, physical layer calculations are only needed for its intended recipient. This returns even bigger computational savings over the Event-Compression abstraction. Additionally, this particular abstraction is less dependent upon the selection of transmit power because only one set of physical layer calculations is performed for each RTS or CTS packet.

2.5 OPNET Validation Model

OPNET Modeler 10.5 [9] was used to validate the results returned by the three data link abstractions. The same parameters and models were used in both simulators wherever possible, usually matched to the OPNET model's default settings, but, due to differences in model and structural design, not all settings are identical. The following provides an overview of the OPNET configuration.

The mobility model and traffic generator in OPNET are configured to behave exactly as described in Sections 2.3.1 and 2.3.2. However, the default mobility model in OPNET does not randomly generate initial locations for nodes. In order to randomize nodes' starting locations, 500 seconds of simulated time are added to the beginning of each OPNET simulation. The collection of medium access layer statistics is delayed until the 500-second startup time has passed.

OPNET's physical layer calculations and transmission handling differ from that described in Section 2.3.3. While OPNET eventually calculates the number of errors in a received packet, it defines the bit error rate as a function of the signal's Signal to Interference and Noise Ratio (SINR) as in (2.7), which reduces to a table-lookup (specific to modulation scheme and data rate) with interpolation to find BER given an SINR level:

$$\text{SINR} = 10\log_{10}\left(\frac{P_r}{I + N_o}\right). \tag{2.7}$$

Here, P_r and I are both calculated using (2.1) and (2.2). The background noise term in OPNET's default noise model is $N_o = 8.80 \times 10^{-14}$ W.

Like the custom simulator, the default OPNET settings fail a packet if one or more error is detected. OPNET calculates the number of errors in a received packet by recording the BER as it changes during the course of transmission (for instance, when another node starts or stops transmitting). For each change in BER, OPNET stores the old BER value and the length of the packet portion transmitted under that specific BER. Upon finishing the packet, each segment and BER measurement is used to compute the total number of errors for the entire packet.

Additionally, OPNET modeled the effects of propagation delay. Differences between our custom simulator and OPNET at the medium access layer are mainly concerned with the transmission of control packets (RTS, CTS, and ACK), which were the focus of our abstractions. In particular, transmitted control packets generated interference and took a non-zero amount of time to transmit (not instantaneous).

2.6 Simulation Results

In this section, data collected from the abstractions and OPNET are presented. At present, we limit ourselves to two representative throughout and delay metrics of the medium access layer, goodput ratio and End-to-End (ETE) delay, while noting that many other metrics are available for measurement and future study.

Goodput ratio is defined as the fraction of goodput over offered load. Goodput, in kbps, is the time rate of bits pushed up from the medium access layer (sum of successfully received packets' sizes over simulation duration). Offered load, also measured in kbps, is the time rate of bits created at the application layer (sum of created packets' sizes over simulation duration).

ETE delay metric essentially measures the time from transmitter to receiver for a one-hop trans-

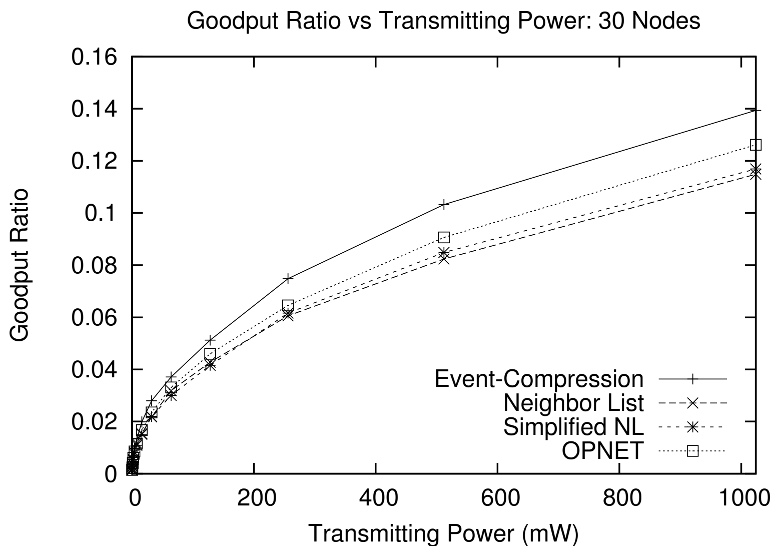

Figure 2.6: The goodput ratio results illustrate the similarity (in trend and values) of the abstracted models to the OPNET model. (Packet inter-generation mean = 1.6 seconds).

mission, which includes queueing delays, medium contention, any propagation delay (if modeled), and transmission delay. The ETE delay is clocked from the moment a packet is sent down to the medium access layer at the source node until the corresponding packet is pushed up by the destination node's medium access layer.

Simulations were set up over a 1 km by 1 km area and individual runs were specified to last for 3600 seconds (1 hour). Data were collected and averaged over 20 independent simulations/runs.

In Figure 2.6, the effects of scaling nodes' transmit power on goodput ratio were recorded for a network size of 30 nodes, a mean packet inter-generation time of 1.6 seconds, and transmit powers from 0.125 mW doubled up to 1024 mW. All four models display the same trend that intuitively suggests nodes can reach a larger portion of the network with a stronger transmission power. This trend should also level off, presumably at the point where nodes are already able to reach the entire network and any benefits from increasing transmit power are negated by the resulting interference generated. Additionally, the low goodput ratios are likely due to random packet destinations combined with the lack of routing, i.e., we do not incorporate multi-hop communication. Overall, the three abstractions show close alignment with the results from OPNET.

Figure 2.7 reveals negligible effects of network size on the goodput ratio curves for the Event-Compression model. For space, the equivalent of the other models' graphs are not included because they illustrate the same behavior.

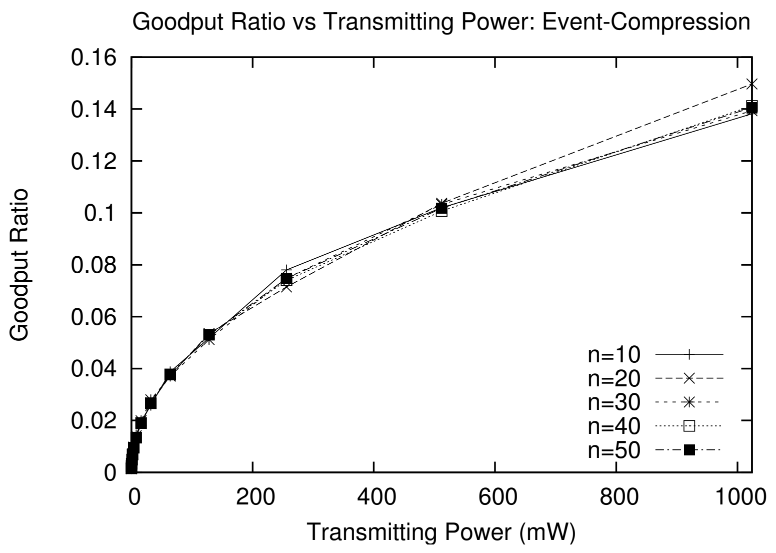

Figure 2.7: The effect of network size on goodput ratio is shown for only the Event-Compression model but reveals the general trend seen in the other models. (Packet inter-generation mean = 1.6 seconds).

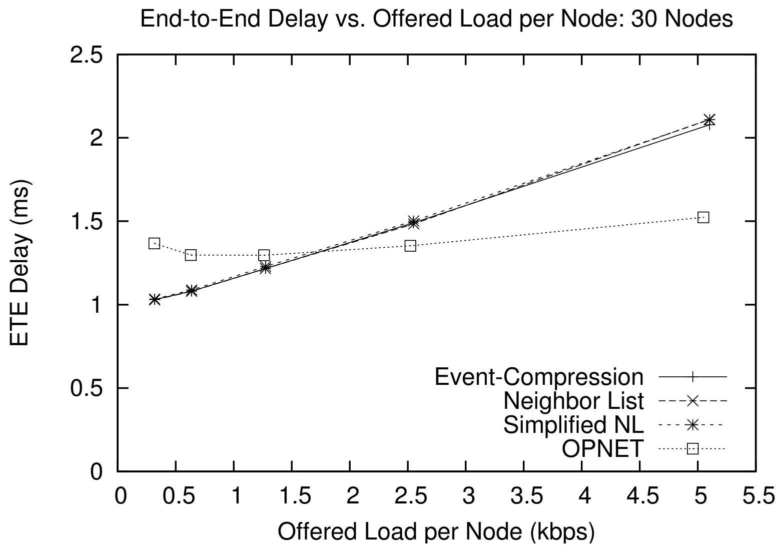

Figure 2.8: The ETE delay measurements show the behavior for all abstracted models and OPNET, producing results of the same magnitude, but differing trends. (Transmit power = 100 mW, packet inter-generation mean = {3.2, 1.6, 0.8, 0.4, 0.2} seconds).

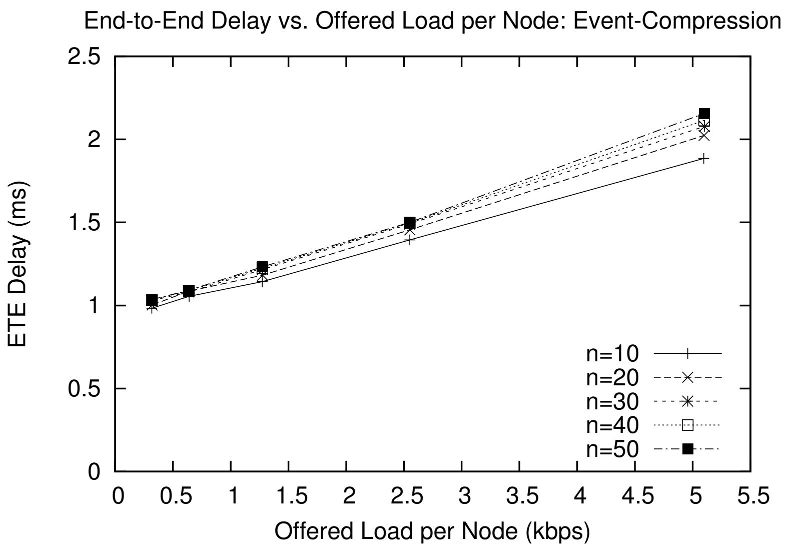

Figure 2.9: The effect of network size on ETE delay is shown for only the Event Compression model, but it conveys the general trend for all models. (Transmit power = 100 mW, packet inter-generation mean = {3.2, 1.6, 0.8, 0.4, 0.2} seconds).

Figure 2.8 displays ETE delay dependency on offered load. The transmit power was fixed at 100 mW while decreasing the mean packet inter-generation time (which has the effect of increasing the offered load per node). In the three abstracted models, ETE delay decidedly increases with the offered load per node. This is supported by the claim that higher offered loads cause more packets to be enqueued at the medium access layer, which in turn creates longer queueing delays. While the abstracted models and OPNET return results of the same magnitude, the latter displays a different trend. This discrepancy is likely rooted in the fact that all three abstractions compressed RTS and CTS events together into an instantaneous transmission, which would have a direct effect on time-based metrics such as ETE delay. In reality, both transmissions take up a finite amount of time and would contribute to the ETE delay measurement.

The second ETE delay plot, Figure 2.9, shows the effect of network size on ETE delay. The Event-Compression model was again chosen to show general model trends by simulating multiple network sizes and offered loads. Transmit power and inter-generation mean are set in the same manner as the other ETE delay simulations. The offered loads are normalized by the number of nodes for comparison between different network sizes. The results indicate that denser networks produce slightly higher ETE delays. Larger network sizes should lead to longer queueing delays due to increased medium contention. Additionally, the relatively close grouping of the Event-Compression

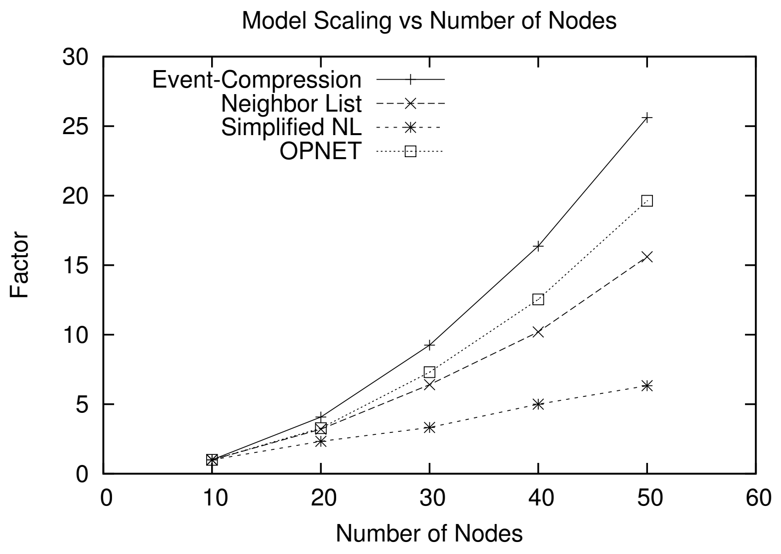

Figure 2.10: The run-time scaling of each model is illustrated. Runtimes are normalized by their respective 10-node simulation runtime. (Packet inter-generation mean = 3.2 seconds).

model's results are indicative of what is seen from the other three models.

Figure 2.10 displays the runtime properties of each model as the number of nodes is increased. Transmit power was set to 100 mW and the inter-generation mean was set to 3.2 seconds. Each model's runtimes are reported as a factor of their respective 10-node runtimes. Thus, for example, Figure 2.10 shows that running a 50-node simulation in OPNET takes approximately 20 times as long as a 10-node simulation in OPNET. Even though the OPNET model scaled better than the Event-Compression model, its absolute runtime was roughly twice as high throughout. Lastly, progression from Event-Compression to Neighbor List to Simplified Neighbor List yields better scaling and roughly translates into a drop from quadratic to linear scaling with network size.

2.7 Conclusion

In this chapter, three abstractions of the IEEE 802.11 RTS/CTS mechanism were detailed. The design of the abstractions sought to decrease scaling of simulation runtime with network size by combining events and reducing the number of receivers considered at the physical layer for control packets. In particular, the 'best' abstraction was the Simplified Neighbor List which achieved near-linear scaling. It was found that all three abstractions yielded goodput ratio results very comparable to the OPNET validation model but contained some discrepancy in the data trends for ETE delay measurements. This discrepancy is likely rooted in the fact that all three abstractions compressed RTS and CTS events together into an instantaneous transmission, which would have a direct effect on time-based metrics such as ETE delay. Future work in this area includes studying additional protocol abstraction methods as well as further developing the notion that different forms of protocol abstraction are best suited for collecting particular data. Such a study would attempt to yield guidelines in choosing the best method given a desired metric.

3. IPv6 Address Autoconfiguration

3.1 Introduction

It has been recognized for several years that address configuration must be streamlined in order to provide rapidly deployable networks for military operations. In particular, it is desired to reduce the level of human intervention - the manual configuration of hundreds (and in some networks, thousands) of devices - which is tedious, time consuming, and expensive. Against this background, the autoconfiguration features in Internet Protocol version 6 (IPv6) appear to have significant potential to simplify the planning and managing of large-scale networks [27–35]. These features were designed so that manual configuration of hosts' addresses before connecting them to the network is no longer needed. Military Mobile Ad hoc Networks (MANETs) can benefit significantly from autoconfiguration features, especially stateless autoconfiguration. However, IPv6 stateless autoconfiguration schemes for MANETs still have to be refined, and be accompanied by a convincing demonstration.

In this chapter, we provide a literature survey of autoconfiguration schemes that could be applied to MANETs. One such proposed stateless autoconfiguration scheme, by Jelger & Noel (J&N) [5], provides globally routable IPv6 prefixes to a MANET that is attached to the Internet via gateways. The J&N scheme is examined here through OPNET [9] simulations, taking into account several extensions beyond what was studied in [5]. First, gateways, which provide connectivity to the Internet or a remote network, are permitted to become mobile. Second, new mobility models are introduced to the nodes so that squad-like clusters are formed around the gateways. Third, the number of ad hoc nodes and the number of gateways are scaled independently. Primary goals of these simulations are to quantify the following trends: (1) the performance of the protocol as the ratio of the number of ad hoc nodes to gateways changes; (2) the scaling of the protocol's overhead and initial autoconfiguration time versus network size; and (3) the protocol's performance under a group mobility regime with various cluster densities.

The developed J&N implementation in OPNET was validated against previous results [5] and also tested in three unique scenarios incorporating the above design considerations. Validation of the J&N protocol produced discrepancies in some performance metrics. Communication with the authors of [5] revealed some simulation configuration differences as potential sources for the discrepancies. In all three of the scenarios, performance of the J&N scheme was found to be highly dependent on network density, and also suggested further protocol refinement before deployment.

The rest of this chapter is organized as follows. Section 3.2 contains an overview of autoconfiguration schemes for MANETs and other related research. Section 3.3 describes the J&N protocol. Section 3.4 presents the motivation for choosing the J&N autoconfiguration protocol and the general networking environment wherein it is applied. Section 3.5 describes the general modeling setup in OPNET - including description of protocols, their parameters, implementation of the J&N protocol, and performance metrics of interest. Section 3.6 explains each of the simulation scenarios. Section 3.7 contains a discussion of trends observed in the simulations. Lastly, Sections 3.8 and 3.9 present conclusions and suggestions for future work respectively.

3.2 Autoconfiguration Approaches and Related Work

Several proposals have been made concerning address autoconfiguration. These proposals can be divided into three main categories: stateful, stateless, and hybrid.

3.2.1 Stateful Autoconfiguration

Stateful autoconfiguration uses address allocation tables to maintain control over assignment of addresses. This method ensures uniqueness of addresses and eliminates the need for Duplicate Address Detection (DAD). However, in order to maintain the allocation table this approach requires either a centralized controller or a synchronized distributed system. Neither centralized control nor synchronized distributed systems are suitable for MANETs. In a centralized scheme [36], the designated Addressing Agent (AA) often incurs large overhead associated with handling and maintaining all addresses for the network. Moreover, a single point of failure is apparent - the entire network depends on a single node which is not guaranteed to be reachable. This lack of robustness can be overcome by using a distributed system, such as MANETconf [37], wherein allocation tables are synchronized across multiple nodes. Some form of reliability assessment must be employed in this case, to ensure that the tables remain synchronized.

3.2.2 Stateless Autoconfiguration

Stateless autoconfiguration allows nodes to self-assign an Internet Protocol (IP) address randomly or based on a hardware identification number. To guard against duplicate addresses, the central element of a stateless proposal is some form of DAD, either active or passive. In Query-based DAD

(QDAD) [27], a node chooses two addresses on startup, a temporary address and a tentative address. The node attempts to establish communication with the tentative address from the temporary address, and then waits a specified period of time. If no response is received, the node assumes that the address is available and adopts it. Unlike QDAD, the alternative methods, Weak DAD (WDAD) and Passive DAD (PDAD), must rely on a routing protocol. In WDAD [28], an initialization key is generated for each node and distributed with all routing packets. The keys are stored in the routing table which is used for comparison with the keys included in subsequent routing packets received. If different keys are received from the same address, then that address is assumed to have been duplicated. In PDAD, proposed by Weniger [29], received routing packets are analyzed to detect any conflicts based on events that would not occur with unique addresses. By using information that is already available in the network, the amount of overhead introduced by this protocol is significantly reduced.

3.2.3 Hybrid Autoconfiguration

Several hybrid approaches have been proposed that use elements from both stateful and stateless autoconfiguration methods. These often provide more robust protocols but also increase complexity and overhead. The Hybrid Centralized Query-based Autoconfiguration (HCQA) [30] protocol uses both QDAD and a centralized allocation table on a dynamically assigned AA. The AA can then prevent duplication even if the original node is offline and not able to respond to the query. The Passive AutoConfiguration for Mobile Ad hoc Networks (PACMAN) [31] protocol employs both PDAD and a distributed allocation table. This protocol does not synchronize the allocation tables actively but allows the nodes to collect the information needed for disambiguation by monitoring routing traffic passively. Additional descriptions of autoconfiguration schemes can be found in [32, 33].

3.2.4 Duplicate Address Detection

Several methods were proposed to prevent duplicate addresses. Most approaches used in centralized stateful autoconfiguration appear to lack the robustness necessary to compensate for the dynamic nature of MANETs and have high network flooding overhead. Approaches used in synchronized distributed stateful autoconfiguration often incur high overhead and falter in the face of high packet loss. QDAD stateless autoconfiguration methods often have high overhead and do not guarantee address uniqueness [27]. They often exhibit difficulties in accounting for network merging and partitioning. Both WDAD and PDAD have to rely on the routing protocol used by the network [28, 29].

It is not clear whether the effort to prevent duplicate addresses preemptively is necessary in many scenarios, since in most reasonable schemes address duplication has a very low probability of occurring. Given a 128-bit address, 64-bit subnet prefix, and random address assignment, there is only a 1 in 2^{64} chance that any two nodes will adopt duplicate addresses. Using a formulation for an upper bound on the probability of address collision in [38], it can be seen that the likelihood of a 10000 node subnet suffering duplicate addresses is less than 5.420×10^{-12}. It appears that in most MANET networks any implemented preemptive DAD mechanism would incur a cost both in complexity and risk of network failure well exceeding the expected benefit of detecting a duplicate address.

3.2.5 MANET Autoconfiguration

The increased interest in using MANETs raises questions about their integration with the Internet. Lamont, et al. [34] discuss an approach to integrate MANETs with the Internet which stresses minimizing handoff latency between Wireless Local Area Networks (WLANs) and MANETs. In [35], "a self-organizing, self-addressing, self-routing IPv6-based MANET which supports global connectivity and IPv6 mobility" is proposed. It uses a global prefix in combination with a logical prefix to form the IP address of mobile nodes. King and Smith [39] discuss the emerging possibility of using an ad hoc network to provide the military with access to distant networks through gateways. They formulate an architecture that includes DAD, two gateway selection schemes (centralized and distributed), and MANET routing protocols. In [40], Ammari and El-Rewini present a method to integrate Internet connectivity to MANETs using mobile gateways. Their work is based on a three-layer approach using Mobile IP and dynamic Destination-Sequenced Distance Vector (DSDV). Denko and Wei [41] present an architecture comprised of multiple mobile gateways in order to connect the Internet to MANETs using an extended Ad hoc On-Demand Distance Vector (AODV) routing protocol. Gateway discovery is presented for both a reactive scheme (for small networks) and a hybrid scheme (for larger networks). In [42], Mo, et al. present new algorithms for connecting MANET nodes to the Internet; these algorithms are independent of routing protocols.

A MANET-Internet autoconfiguration scheme of particular interest is that of J&N [5]. Their focus is on the autoconfiguration of globally routable IPv6 addresses in an ad hoc network that is connected to the Internet via one or more gateways (i.e., a hybrid ad hoc network). The J&N

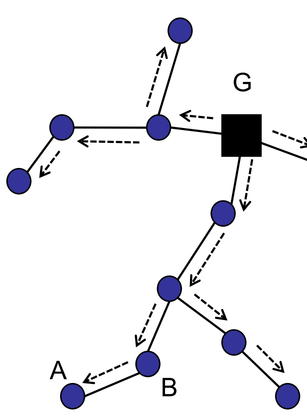

Figure 3.1: An example prefix tree formed from gateway G.

protocol forms logical trees anchored at the gateways; the branches consist of ad hoc nodes that have selected the same prefix as the gateway. A simple example is shown in Figure 3.1. Each ad hoc node that has selected a gateway, has a path to that gateway such that all intermediate nodes and the gateway share the same global prefix. This property is called prefix continuity. Some of the benefits of prefix continuity are the avoidance of source routing, as the sender of a packet does not have to specify entire routes in the packet header, and support for a dynamic network topology that includes network partitioning, merging, and temporal gateways [5].

3.2.6 Military Networks and Mobility Models

Several studies used simulations in order to understand how IPv6 operates in hierarchical military networks. Military network representation is perhaps best exemplified in [43], where the use of an IPv6 MANET of tactical radios is explored. Other studies that dealt with military network topology include the work of Kant et al. [44], though their study does not focus on IPv6.

Most simulations use a Random Waypoint (RWP) [23] scheme to represent node placement and movement. This approach has been criticized in the literature (e.g., [24]). In the context of the objectives in this chapter, traditional RWP often fails to represent a realistic mobile scenario, as it is unlikely that all nodes in a military network would wander about in a manner conforming to the distributions assumed by RWP algorithms. It is much more reasonable to assume that nodes in military networks move in a coordinated scheme or are at least organized in groups and clusters.

3.3 Prefix Continuity

The J&N protocol is dependent on one major mechanism and a second, optional mechanism. The protocol's major mechanism controls how globally routable prefixes are advertised and selected, in order to ensure prefix continuity. Gateways periodically advertise their global prefixes in messages known as Gateway Information (GW_INFO) messages. These advertisements are sent out at an interval measured in seconds specified by the variable gw_info_refresh_period. GW_INFO messages contain such fields as the gateway (global) prefix advertised and distance to the gateway measured in hops.

If a node receives a GW_INFO message and decides to accept the advertised gateway's prefix, the sending node becomes the upstream neighbor of the receiving node. Nodes will only forward GW_INFO messages containing an advertised prefix that matches their selected gateway. By traveling along the path of upstream neighbors recursively, one will eventually reach the gateway that advertised the prefix that all the traversed nodes adopted. This forwarding process is key to producing prefix continuity. In Figure 3.1, node A has chosen node B as its upstream neighbor. Lines in the figure indicate wireless connectivity and the arrows show the paths of the forwarded GW_INFO message from gateway G.

Over the course of time, ad hoc nodes in the network may receive advertisements originating from multiple gateways, and must decide which gateway to select. Figure 3.2 shows a scenario in which node A receives multiple forwarded advertisements from its surrounding neighbors B, C, and D. J&N provide several algorithms for selecting an upstream neighbor, the two most significant being the *distance* and *stability* algorithms. A node operating under the distance algorithm will change its selected global prefix if the distance in hops from itself to a newly advertised gateway is less than the distance to the current gateway; this is done in an attempt to maintain a minimum distance to the Internet (via the selected gateway). Referencing Figure 3.2, node A would select the prefix of gateway $G1$ and choose B as its upstream neighbor. The stability algorithm seeks to maximize the amount of time spent with the same prefix and will not change gateways as long as it continues to receive GW_INFO messages advertising its currently selected prefix. When selecting a new gateway and upstream neighbor, nodes choose the global prefix that was advertised by the largest number of nodes, and an upstream neighbor that minimizes the distance to the chosen gateway. If node A (Figure 3.2) was using the stability algorithm and needed to choose a new gateway, it would select the prefix of $G2$ due to the number of neighbors forwarding $G2$'s advertisements. Node A would

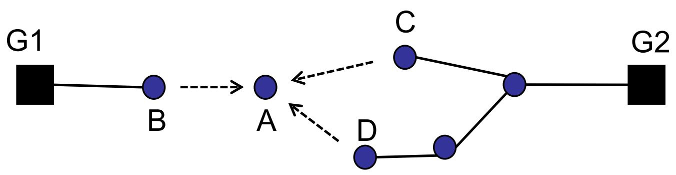

Figure 3.2: An example network with two advertising gateways, $G1$ and $G2$.

then choose C as its upstream neighbor because it is the closest (out of nodes C and D) to gateway $G2$.

A second, optional mechanism exists to verify bi-directionality in the wireless links between nodes. Under some circumstances, such as heterogeneous devices or wireless channel characteristics, links between nodes may be uni-directional. In these situations pairs of nodes may perform a three-way handshake using Bi-directional (BIDIR) messages before one node can choose the other as its upstream neighbor.

In the J&N scheme, each node maintains a neighbor table built from the GW_INFO and BIDIR messages received. These tables assist in the selection of new upstream neighbors. The table entries are set to expire if not refreshed by incoming GW_INFO messages. For more details on the J&N protocol, please see [5, 45, 46].

3.4 Network Environment

The J&N prefix continuity protocol is applied to a more complicated environment than the scenario studied by the original authors, namely, one that better approximates a military network topology. In their original study, J&N address the performance of their protocol in a fixed-size (100 nodes) ad hoc network with four (4) stationary gateways placed in the corners of a simulation arena (2000 m x 2000 m). The ad hoc nodes were permitted to move about the entire simulation space according to a RWP mobility model.

The original setup is unsuitable for the networks of immediate interest. First, it may not be reasonable to expect the placement of gateways to bound a geographical region enclosing a MANET. Second, J&N only present the study of a fixed-size, 100 node network, therefore the scalability of the protocol is unclear. Autoconfiguration protocols that run on military networks (consisting of hundreds to thousands of nodes with varying densities) must be scalable with regard to autoconfiguration time and protocol overhead. Third, military networks may consist entirely of mobile nodes, including mobile gateways. Finally, platforms in military networks are not likely to be traveling randomly about an entire geographical region; movement is always coordinated to some extent.

In applying the J&N protocol to a military-type network, Internet connectivity could be easily equated with connectivity to a larger or remote network. Specifically, a hierarchal MANET is considered and is illustrated in Figure 3.3, consisting of two types of platforms, labeled leaders and subordinates. The set of leader platforms form a global MANET subnet, which can be considered a wireless backbone. Leader platforms and geographically close subordinate platforms produce additional wireless local MANET subnets. The gateway-node relationship from J&N is applied directly to the leader-subordinate analog here.

Additionally, a group mobility model is considered for the subordinates. It encourages cluster formation around the gateway nodes to better mimic squad-like military formations. Further, a simple random waypoint movement scheme is assumed for the gateways. Mobile gateways introduce additional events of interest, such as when two gateways that publish different global prefixes approach each other. It is important to observe how surrounding ad hoc nodes react to moving gateways in close proximity.

Leader platforms contain two wireless interfaces, one for longer range communication with other leaders, and one for local communication with subordinates. Subordinate platforms have only one wireless interface for communication between local subordinates and gateways.

Leader platforms are assumed to be preconfigured in a manner that allows stable communication among leaders, and the focus of this study is placed on the autoconfiguration of subordinate platforms. All leaders publish their prefixes to surrounding subordinates in order to establish the logical prefix trees associated with prefix continuity as described earlier.

The prefix continuity protocol does not make any assumptions about the underlying ad hoc network topology or the number of gateways. In fact, the ad hoc network may be comprised of multiple partitions (each with one or more gateways) and still operate successfully. For military networks these properties provide flexibility in the way subordinates and leaders are arranged. For example, leaders may come online, disappear, or move to a new location; subordinates will have to adjust.

Ad hoc nodes that stray too far from their affiliated gateway will re-associate with a more appropriate gateway (if available); otherwise they become ‘orphaned’. Re-association is accomplished through the upstream neighbor selection algorithms.

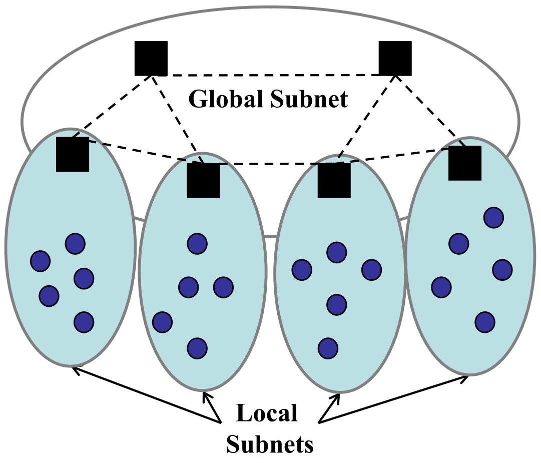

Figure 3.3: The logical network topology under consideration. Leaders, denoted by squares, form the backbone and serve as attachment points for the subordinates, represented as dots.

3.5 General Simulation Details

This section details the general scenario representation in OPNET Modeler version 12.0 [9]. Parameter values specific to a particular scenario, as well any exceptions to the general model setup described are detailed later. Where possible, simulation parameters were set to values equal to those used in the J&N study [5].

The simulation arena was a flat 2000 m by 2000 m square. N_{ah} is used to designate the total number of ad hoc nodes in the simulation arena, while N_{gw} represents the number of gateways. Gateway and ad hoc nodes were built from the standard OPNET 'manet_station_adv' node model. Since the wireless backbone formed by all leaders was not the focus of this particular study (and therefore not actively simulated), gateways and ad hoc nodes each had only one Institute of Electrical and Electronics Engineers (IEEE) 802.11 interface.

The default wireless propagation model in OPNET used the Friis transmission equation (2.1) as shown in Section 2.3.3. The equation parameters were set such that a transmission had a maximum range of 250 m under interference-free conditions. The transmitter and receiver antenna gains were assumed to be isotropic and were both set to 0 dB. The pathloss exponent was set to 2 to reflect free-space propagation, and the default OPNET noise figure of $N_o = 8.80 \times 10^{-14}$ W was used. A transmission power of 0.2 mW and receiver sensitivity of -95 dBm was used to force the 250 m distance limit on transmissions - if the received signal power was less than the receiver sensitivity, the transmission was immediately considered unsuccessful. Transmissions were also subjected to

Signal to Interference and Noise Ratio (SINR) calculations using equations (2.2) and (2.7). Finally, as discussed in Section 2.5, OPNET maps the SINR to a Bit Error Rate (BER) depending on the modulation scheme in use by IEEE 802.11, and is configured to fail a transmission if any bit errors are detected.

Application traffic was not modeled in the network. A 'warm-up' time of 3000 seconds was applied to the mobility models so that the spatial distribution of nodes approached steady-state [24], after which the J&N protocol was started and statistics began to be recorded.

3.5.1 Prefix Continuity Model

A model of the J&N prefix continuity protocol was constructed in OPNET based on [5,45,46]. It was implemented as a stand-alone process model (i.e., not integrated with a specific routing protocol) and interfaced with the User Datagram Protocol (UDP) transport layer protocol. BIDIR messages were disabled, as all nodes used the same transmission power. Both the stability and distance algorithms for upstream neighbor selection were studied. Prefix continuity protocol parameters, which controlled timers and neighbor table entry timeout values, were set in accordance with [45].

3.5.2 Mobility Models

Mobile gateways were permitted to move about the entire simulation space according to a RWP model [23] with a constant speed of 2.5 m/s and a pause time of 25 seconds.

Ad hoc nodes were assigned a group mobility model that consisted of a restricted RWP model. At the beginning of the simulation, each node chose a random gateway uniformly from the set of all gateways. The restricted RWP selection algorithm would choose waypoints within a specified region of the chosen gateway. The destination selection was controlled by the parameter xy_var, which specified the maximum coordinate deviation in meters in both the horizontal and vertical directions from the chosen leader. Ad hoc nodes moved at a constant speed of 5 m/s and had a pause time of 10 seconds. See Figure 3.4 for a visualization of this setup.

Under this mobility model, orphaned nodes may be caused if xy_var is too large, permitting the ad hoc nodes to stray too far away from available upstream neighbors, or if N_{ah} is too small, limiting the number of potential upstream neighbors.

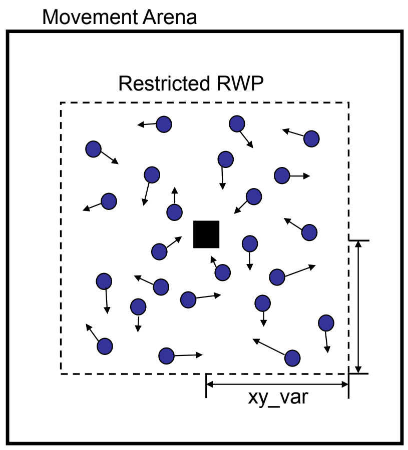

Figure 3.4: Ad hoc nodes (blue circles) are restricted to choosing waypoints within the vicinity of their leader (black square).

3.5.3 Performance Metrics

In this section, the performance metrics collected from the simulations are defined; many of them were proposed in [5].

- **Total Autoconfiguration Time (seconds)** - The elapsed time between the transmission of the first GW_INFO message and the time that 95% of the total number of ad hoc nodes had selected their first global prefix.
- **Autoconfiguration Overhead (bytes/second per node)** - The node-average rate of data passed down from the J&N protocol to the UDP process. This does not include IPv6 or Medium Access Control (MAC) headers.
- **Prefix Updates (updates/node)** - The node-average number of prefix updates that a node experiences during simulation. A prefix update occurs when an ad hoc node chooses a new upstream neighbor but retains the same global prefix.
- **Prefix Changes (changes/node)** - The node-average number of prefix changes that a node experiences during the simulation. A prefix change occurs when an ad hoc node chooses a new upstream neighbor and global prefix.
- **Average Prefix Hold Time (seconds)** - The node-average period during which a prefix remained constant for any given ad hoc node. The prefix hold timer started upon configuration

of a new prefix and stopped for only the following events: a prefix change occurred, or the upstream neighbor entry timed out.

- **Percentage of Time Without a Prefix (%)** - The node-average percentage of time a node spent without a prefix, starting from the transmission of the first GW_INFO message until the end of the simulation.

3.6 Simulation Scenarios

In this section, we describe a validation scenario as well as three new scenarios (shown in Figure 3.5) used to capture the performance of the prefix continuity protocol. The primary goals of these new scenarios are to quantify the following trends: (1) the performance of the protocol as the ratio of the number of ad hoc nodes to gateways changes; (2) the scaling of the protocol's overhead and initial autoconfiguration time versus network size; and (3) the protocol's performance under a group mobility regime with various cluster densities. Each scenario combination was run ten (10) times. All data presented is averaged over the 10 runs.

3.6.1 Validation Scenario

We first validated our OPNET implementation with J&N's data. To this end, the scenario presented in their original paper [5] was replicated. J&N's simulation arena consisted of a flat 2000 m by 2000 m area with a stationary gateway placed in each corner, 250 m away from each edge. Each gateway advertised a unique prefix. One hundred nodes moved about the simulation space according to random waypoint with speeds chosen uniformly from the range [0.5, 1.5] m/s and pause times of 150 seconds. Simulations of this scenario were run for both upstream neighbor algorithms. Each simulation run lasted 65 simulated minutes (50 minutes for mobility model 'warm-up' time plus 15 minutes of protocol operation).

3.6.2 Scenario I: Single, Stationary Gateway

The first new scenario examined the effect of scaling the number of ad hoc nodes, N_{ah}, for a single stationary gateway ($N_{gw} = 1$) located at the center of the (square) simulation arena. This scenario helps shed light on how the prefix continuity protocol behaves in the presence of larger and more dense networks. N_{ah} was varied from 25 to 400 nodes. For each ad hoc network size, the group mobility parameter xy_var was varied from 250 to 1000 meters so that the ad hoc

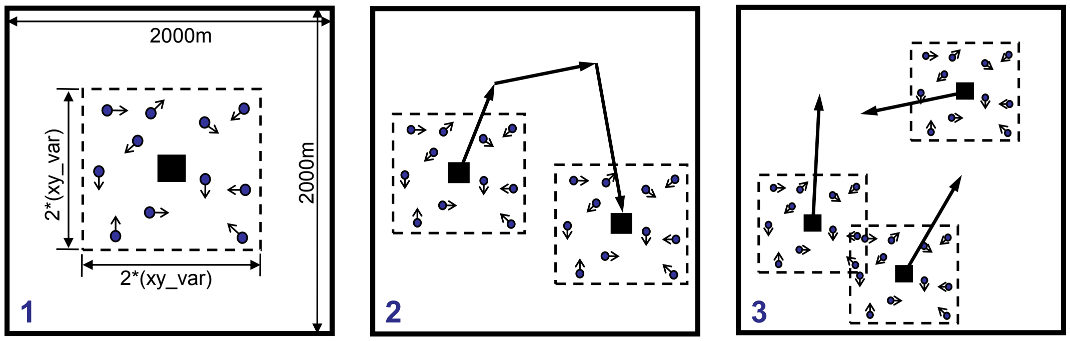

Figure 3.5: Scenarios I-III are shown from left to right.

nodes movement became less dependent on the chosen leader. Only the distance upstream neighbor selection algorithm was studied under this scenario (the stability algorithm simplifies to the distance algorithm in the presence of only one advertised prefix). Each simulation run lasted 65 simulated minutes (using the same warm-up/operation division as in the validation section).

3.6.3 Scenario II: Single, Mobile Gateway

The second scenario studied the effect of gateway mobility for a single gateway ($N_{gw} = 1$). N_{ah} and xy_var were varied as in Scenario I. The gateway node was configured to move around the simulation arena under the unrestricted random waypoint model described in Section 3.5. Again, only the distance algorithm was simulated in this scenario. Each simulation run lasted 75 simulated minutes (adding 10 extra minutes to the protocol operation).

3.6.4 Scenario III: Multiple, Mobile Gateways

Finally, multiple gateways were permitted to move without restriction in the simulation space for the third scenario. The number of gateways, N_{gw}, was varied from 1 to 4. Each gateway was set to advertise a unique global prefix. For each selection of N_{gw}, several values for the ad hoc network size, N_{ah}, were tested while xy_var was fixed at 500 m. Each simulation run lasted 75 minutes, as in the previous scenario.

3.7 Simulation Results

In general, the OPNET implementation of the J&N protocol performed as expected and was comparable to the data presented in [5], including autoconfiguration time, prefix updates, prefix changes, and prefix hold time. For data relating to the autoconfiguration time ('convergence' in [5]), prefix changes per node, and prefix updates per node, similar trends were found for both upstream neighbor selection algorithms. However, there was a difference in the reported average prefix hold time. Our OPNET simulations reported an average prefix hold time on the order of ten (10) seconds for both upstream neighbor algorithms, while J&N reported average prefix hold times on the order of one hundred (100) seconds for the stability algorithm.

After discussion with the original authors, it was found that our OPNET validation scenario did not include stationary relay nodes that were used to increase the effective transmission range of the gateways in [47]. These nodes served to counteract the RWP steady-state distribution of node positions, located around the center of the simulation arena. The lack of relay nodes made it easier for the gateways to become disconnected from the MANET, potentially driving the OPNET-measured prefix hold times lower.

Other potential sources for these differences include inherent differences in the simulators [15] (J&N used the network simulator, ns-2, in [5]) and differences in the interpretation of how the metric should be measured.

3.7.1 Scenario I: Single, Stationary Gateway

Figures 3.6 and 3.7 address the scaling of the total autoconfiguration time and the prefix continuity protocol overhead, as the number of nodes in the ad hoc network increases around a single, stationary gateway for various cluster sizes (controlled by xy_var).

Figure 3.6 shows the total autoconfiguration time (in seconds) versus the number of ad hoc nodes in the network, while the cluster size variable, xy_var, serves as a parameter. The measured autoconfiguration times show a strong dependence on the density of the cluster around the gateway. The density of the network can be increased in two ways: by adding more ad hoc nodes (N_{ah}) to the network, or by making the cluster area smaller, via xy_var. In both cases, the autoconfiguration times decrease for more dense networks. This is largely attributed to nodes already being within range of a potential upstream neighbor in order to autoconfigure for the first time. In less dense networks, more time is spent waiting for nodes to move within range of potential upstream neighbors, and a larger total autoconfiguration time is recorded.

Figure 3.7 shows the overhead per node (in bytes/second) versus the number of nodes, N_{ah}, in the ad hoc network, while xy_var serves as a parameter controlling the cluster area. Increasing the density of the cluster around the gateway, either by increasing N_{ah} or by decreasing xy_var, tends to

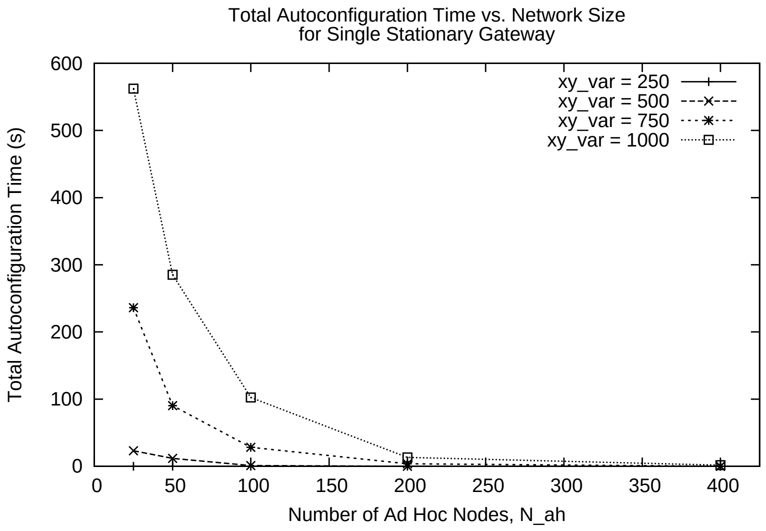

Figure 3.6: Total autoconfiguration time plotted against the number of ad hoc nodes for varying group mobility parameter values. At the plotted scale, the curve for $xy\_var = 250$ lies very close to the horizontal axis and is not visible.

produce higher overhead in simulation. This behavior is explained by the connectivity of the network and the GW_INFO forwarding process. As the network becomes denser, a greater percentage of ad hoc nodes are connected to the gateway via one or more hops and will participate in the GW_INFO forwarding process, occurring once every gw_info_refresh_period.

However, the specific curve for $xy\_var = 250$ m in Figure 3.6 is nearly level, showing that adding ad hoc nodes to the network has little effect on the protocol overhead. Under this specific operating region, the network has already reached full connectivity and that most, if not all nodes are already participating in the GW_INFO forwarding process every gw_info_refresh_period.

3.7.2 Scenario II: Single, Mobile Gateway

Figures 3.8 and 3.11 present the performance of a single, mobile gateway. Average prefix hold time (Figure 3.8) and fraction of time without a prefix (Figure 3.11) of the prefix continuity protocol are shown. Both metrics are plotted against the number of nodes in the ad hoc network, while the cluster size variable, xy_var (in meters), serves as a parameter.

Examining the prefix hold time curves in Figure 3.8 shows two relationships between prefix hold time and the control variables. For a fixed cluster area size, Figure 3.8 displays a decrease in prefix hold time as more ad hoc nodes are added to the network. Figure 3.9 sheds some insight into this

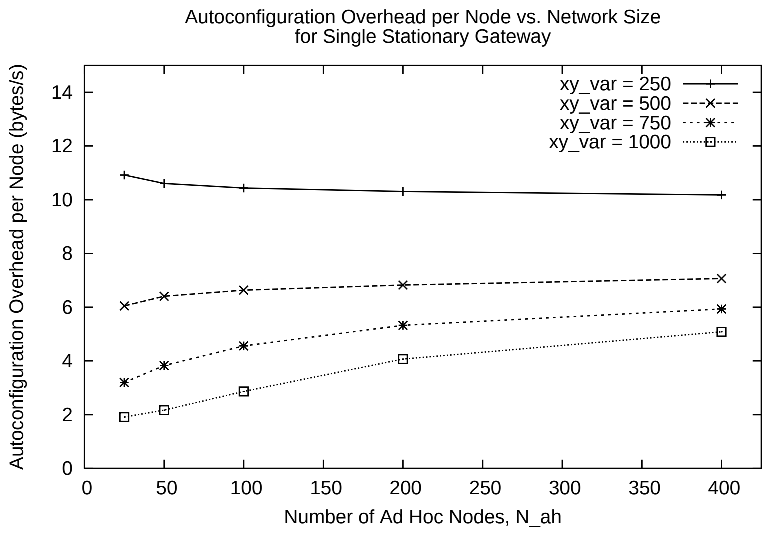

Figure 3.7: Autoconfiguration overhead shown versus the number of ad hoc nodes for varying group mobility parameter values.

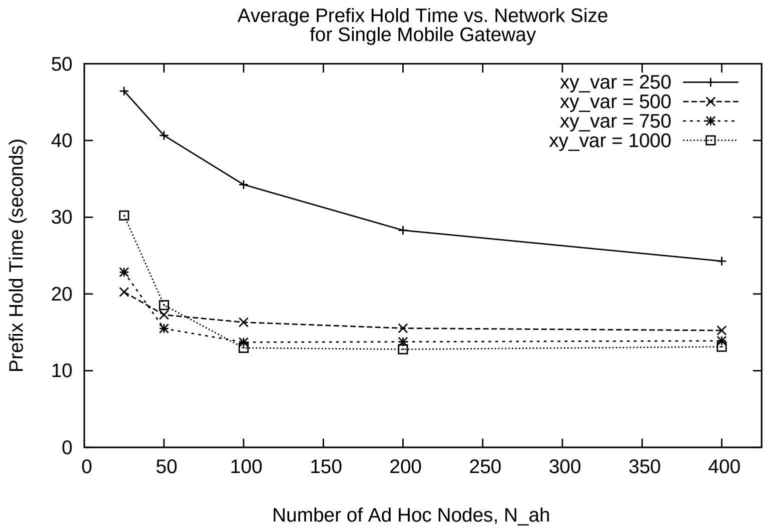

Figure 3.8: Average prefix hold time per node plotted against the number of ad hoc nodes for varying group mobility parameter values.

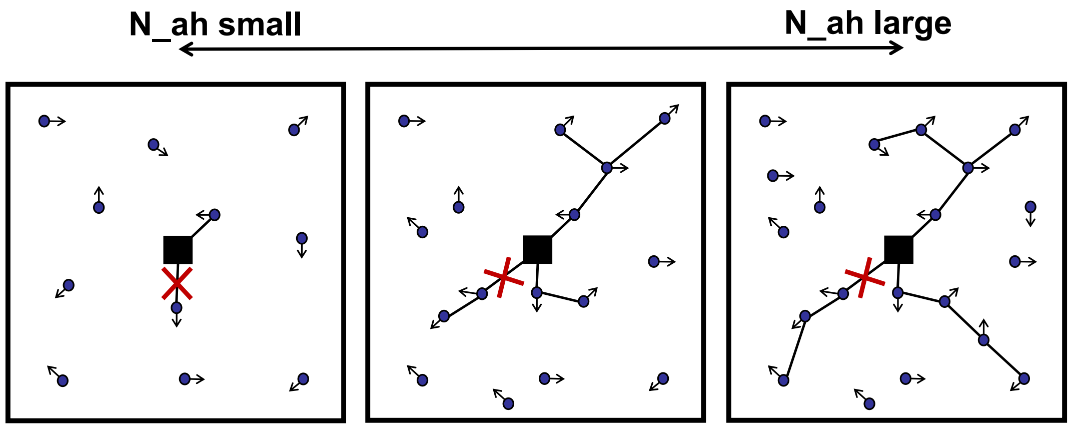

Figure 3.9: For a fixed cluster area size (xy_var), adding more ad hoc nodes (N_{ah}, circles) promotes longer logical prefix branches.

trend by illustrating that longer logical prefix branches are more easily formed in dense networks. However, the prefix branches can be fragile, and the disconnection of an ad hoc node near the root of a branch affects the prefix hold times for all downstream nodes, driving the average prefix hold time down. Thus, larger network sizes that promote longer logical prefix branches contribute to lower average prefix hold times.

Similarly, for a fixed number of ad hoc nodes in the network, Figure 3.8 shows that the average prefix hold time generally decreases as the cluster area size is increased (via xy_var). The left and middle example networks in Figure 3.10 illustrate the effect of increasing the cluster area size on the formation of logical prefix branches. The lengths of logical prefix branches that are possible increase as the diameter of the network changes due to xy_var. The longer logical prefix branches that result from larger xy_var values lead to lower average prefix hold times for the same reason described in the preceding paragraph. The exception to this trend occurs for very sparse networks (*e.g.*, $N_{ah} = 25$ nodes and $xy\_var = 1000$ m). The few nodes that actually configure a prefix (and consequently report to the average prefix hold time metric) do so usually directly from the gateway. Due to the sparsity of the network, multi-node prefix branches are unlikely to form (the rightmost example network in Figure 3.10), and do not have the opportunity to drive the average prefix hold down as previously argued. The end result is that very sparse networks tend to report higher prefix hold times than the other network configurations, as seen in Figure 3.8.

Figure 3.11 shows that the percentage of time without a prefix is highly dependent on the density of the network. Increasing the network density through N_{ah} or xy_var will result in lower

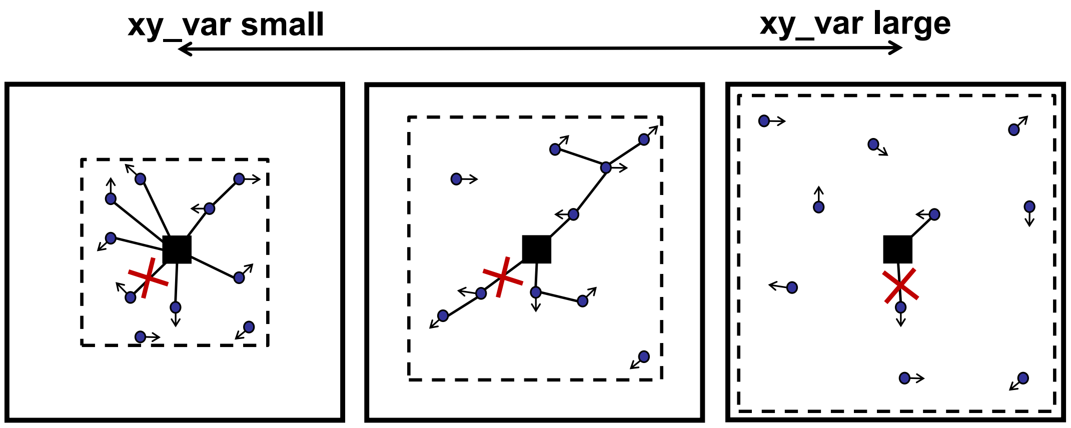

Figure 3.10: For a fixed number of ad hoc nodes (N_{ah}, circles), increasing the cluster area size (xy_var, dashed box) promotes longer logical prefix branches until the network becomes too sparse.

percentages of time without a prefix. By increasing network density, ad hoc nodes are more likely to be connected to a logical prefix branch at any given time. It is also interesting to note that just because a particular network configuration may report a high average prefix hold time, such as the extremely sparse network from the previous discussion, it does not mean that the nodes experience a low percentage of time without a prefix. In fact, for the case where there were the fewest ad hoc nodes, $N_{ah} = 25$, in the largest cluster size, $xy\_var = 1000$ m, the percentage of time without a prefix is extremely high. This supports the previous assertion that most nodes are too far away from upstream neighbors to configure a prefix and the few nodes that do configure a prefix usually do so from the gateway directly.

Figures 3.8 and 3.11 together show that even though the average prefix hold time decreases with network size, the percentage of time the average node spends without a prefix also decreases. The same metrics from Scenario I, not shown, show the same data trends. When data from Scenario I and II were directly compared, they indicated that gateway mobility tends to lower the average prefix hold time, increase the percentage of time without a prefix, and make the logical prefix branches harder to maintain.

It is also prudent to note that the absolute measure of some performance metrics may be at unacceptable levels for use in a MANET environment. Excessively low prefix hold times could disrupt transport layer sessions to the point that certain applications become unusable. For example, the average prefix hold times shown in Figure 3.8 are never higher than 60 seconds, which may prove to be detrimental to an File Transfer Protocol (FTP) session. This suggests that the protocol still

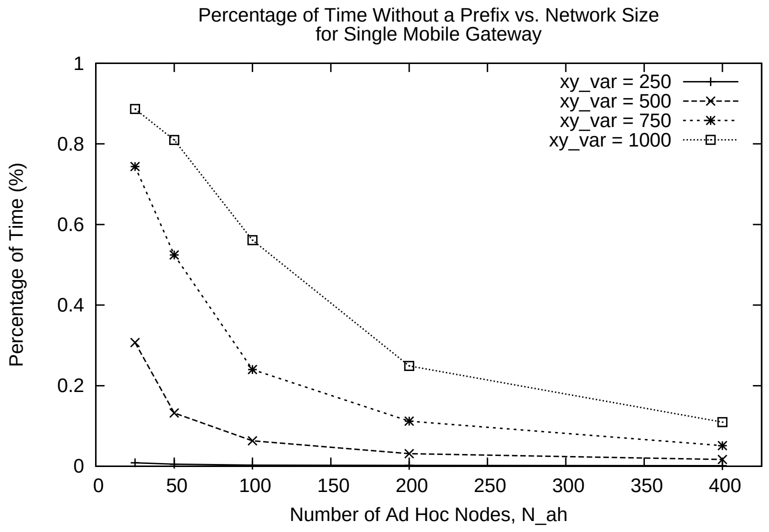

Figure 3.11: Percentage of time without a prefix per node plotted against various node densities.

needs to be refined and adjusted to increase average prefix hold time performance.

3.7.3 Scenario III: Multiple, Mobile Gateways

Figure 3.12 displays both the prefix updates per node (left vertical axis, marked as UP in the legend) and the prefix changes per node (right vertical axis, marked as CH in the legend), and plotted against the number of gateways, N_{gw}. Prefix updates and changes are shown for the distance and stability upstream neighbor selection algorithms, marked with initials D and S respectively in the legend. The plot is shown for an ad hoc network size of 200 nodes and $xy\_var = 500$ m, as the data demonstrated similar trends for the other network sizes.

As seen in Figure 3.12, the number of prefix updates for both algorithms decreases as gateways are added. This tendency is due to the increased partitioning of the 200 ad hoc nodes, causing smaller groups of nodes to form around each gateway. Conversely, the number of prefix changes increases for both algorithms (albeit very little for the stability algorithm) as the number of gateways increases. This tendency is attributed to the fact that each gateway advertises a unique prefix. By making more prefixes available in the network, it is more likely that nodes will experience prefix changes during the simulation.

Comparing the two algorithms in Figure 3.12, the stability algorithm was found to produce more prefix updates and fewer prefix changes than the distance algorithm. This tendency is due to the

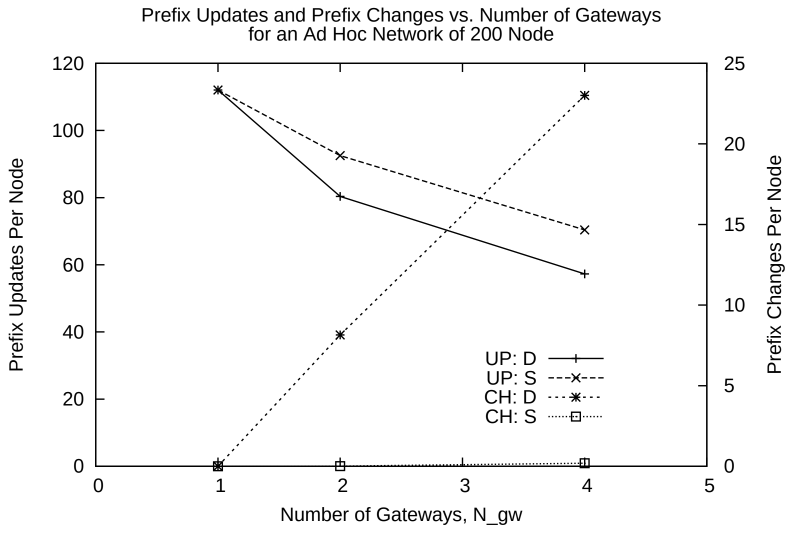

Figure 3.12: Number of prefix updates (left axis) and prefix changes (right axis) versus the number of mobile gateways.

way each algorithm selects upstream neighbors. The stability algorithm attempts to minimize prefix changes by choosing upstream neighbors that preserve the current prefix; the distance algorithm chooses an upstream neighbor solely on the distance (in hops) of that neighbor to the advertised gateway.

In terms of the performance metrics discussed for previous scenarios, the act of adding more gateway nodes to the overall network had the general effect of decreasing the density of each cluster (consisting of one leader and an equal portion of the ad hoc nodes). For example, a network of 4 gateway and 200 ad hoc nodes is broken down into 4 clusters, each consisting of 1 leader and (on average) 50 ad hoc nodes. The act of adding gateways to the network increased the total autoconfiguration time, decreased the average prefix hold time, and increased the fraction of time with a prefix.

3.8 Conclusions

The performance and scaling properties of an IPv6 stateless address autoconfiguration scheme, the J&N prefix continuity protocol [5], as applied to military-type MANETs was investigated. Initially, the OPNET protocol model was validated against the original data [5] to ensure proper operation. In terms of most metrics, simulation results displayed the same trends as those of [5].

However, there were noted differences in prefix hold times with several potential sources for such differences. Next, the scalability of a single, stationary gateway was examined. Subsequently, focus was placed on protocol performance under a single, mobile gateway. Finally, general performance characteristics were gathered when multiple mobile gateways were present in the network.

In the single stationary gateway scenario (Scenario I), large network densities achieved rapid autoconfiguration times. Although the autoconfiguration overhead was higher for dense clusters, the overhead in general was very low when BIDIR messages are disabled. Hence the protocol shows potential for military networks where bandwidth availability is a concern and routing protocols can validate bi-directionality in links.

By permitting gateways to move in a simple random waypoint scheme in Scenario II, the protocol's performance was impacted. Gateway mobility increased the percentage of time without a prefix and decreased the prefix hold time. It was found that adding more ad hoc nodes to the network tended to decrease the percentage of time without a prefix as well as the prefix hold time, suggesting a tradeoff to be investigated further. The low prefix hold time measurements in general suggested that ad hoc nodes may experience difficulties in maintaining higher layer sessions. The J&N protocol may need be revised further to improve performance in this area.

Allowing multiple clusters to move around freely in the arena enabled the observation of how the two neighbor selection algorithms handled gateway mobility. The stability algorithm resulted in a multitude of prefix updates and very few prefix changes, as it was designed to maximize average prefix hold time. The distance algorithm registered more prefix changes per node as a result of its focus on minimizing distance (in hops) to the chosen gateway. Additionally, it was observed that adding more gateways effectively lowered the network density for each cluster, yielding changes in performance that conformed to results from the previous scenarios.

3.9 Future Work

Future studies should address the feasibility of a hierarchical layering of the prefix continuity protocol, such that mobile gateways would first autoconfigure their prefixes from one or more status-elevated gateways. Autoconfiguration of the ad hoc nodes underneath would then take place after a gateway completed its own autoconfiguration.

Allowing multiple gateways in the same mobile group to advertise the same prefix is another scenario of interest. This capability could provide faster autoconfiguration time while possibly also increasing prefix stability.

Third, it is worthwhile to investigate the performance of the prefix continuity protocol in light of the ‘parking lot’ problem. A network may specifically autoconfigure in a static topology, or ‘parked’ state, and mobilize afterward.

Attention should also be given to the notion of an optimal gateway-to-ad hoc node ratio. Such a study should seek to find a threshold where the selected number of gateways balance metrics such as percentage of time without a prefix and prefix hold time.

4. Simulation Cross-Validation of Emulation Testbed[*]

4.1 Introduction

Accurate performance prediction and testing of communications devices and protocols before deployment and standardization is a necessity. Implementation bugs and poor designs that are passed on to consumers discourage adoption and success in the marketplace. Certain scenarios, such as tactical military deployments and rescue operations, are far less forgiving when it comes to operational errors of communications technology. Network simulation and emulation are two common tools used during development to catch and fix such flaws in design and implementation. These tools provide independent methods of validating the performance of new protocols, as well as provide feedback on correct protocol implementation and configuration.

While simulation and emulation are in and of themselves very useful, each offers advantages that cover shortcomings of the other. Discrete event simulations can offer extensive debugging and event control capabilities as well as reproducible sequences of events. Emulation testbeds, which typically run live implementations at the network layer and above on top of emulated links (substituted medium access and physical layers), cannot so easily stop and step through time. Furthermore, emulations are locked into a 1:1 'real-time' run time, which is not the case for simulations. Depending on the complexity of simulation models, faster than real-time results can be collected and analyzed, which is important for long duration experiments. Additionally, scaling simulations to study large networks is much more cost effective than using an emulation testbed. However, it has been argued that emulation testbeds offer more realistic network behavior than simulations [3] due to the fact that actual implementation code is run on network devices. Relying on simulation alone may in fact hide design flaws in the protocols due to code or hardware differences, that would otherwise be revealed when emulating the same network [1]. Instead, using both methods together to study network protocols builds confidence that the protocols in question are configured and operating correctly.

Recent work in the Internet Engineering Task Force (IETF) has produced three proposed extensions to the Open Shortest Path First version 3 (OSPFv3) routing protocol that are better suited for

[*]This work was done while J. Wildman was an intern at MIT Lincoln Lab over the summer of 2007. Constructive and helpful guidance was provided by both supervisor, Dr. Siamak Dastangoo, and fellow intern, Dr. Glenn Carl. Duties included development and management of simulations in support of Dr. Carl's emulation testbed experiments.

the lower data rate and dynamic topology of Mobile Ad hoc Networks (MANETs) [48–50]. These extensions are prime candidates for comparative studies using simulation and emulation methods as they are new and still in development. This chapter details an effort to study and compare different operating modes of one of the OSPFv3 extensions, called MANET Designated Router (MDR), in both a simulation and emulation environment. The measured Open Shortest Path First (OSPF) overhead from both environments was used as a benchmark to construct equivalent MANET representations and protocol configuration, made particularly challenging due to the wired nature of the emulation testbed. During the process of results matching, limitations of the simulated implementation of OSPF were revealed.

Within this chapter, particular attention is given to the simulation environment, as extensive details on the setup and experimentation process of the emulation testbed setup are provided in [7]. Section 4.2 provides background on the OSPFv3 protocol and its proposed MDR extension. Section 4.3 introduces the different environments and OSPF implementations (OPNET simulation and emulation testbed) being cross-validated. Section 4.4 details the efforts involved in the construction of equivalent simulation and emulation environments. Section 4.5 compares the simulation performance results to the emulated testbed. Sections 4.6 and 4.7 present the conclusions and provide future directions of work, respectively.

4.2 Background on Open Shortest Path First (OSPF)

OSPF is a widely used link-state driven routing protocol. Development and standardization of the protocol has spanned roughly two decades and has generated three versions, starting with the formation of the IETF OSPF working group in 1987 and continuing with OSPFv3 and its numerous extensions as of the time of this writing.

OSPFv1, which quickly evolved to OSPFv2, was designed for Internet Protocol (IP)v4 networks. The last Request for Comments (RFC) released for OSPFv2 was RFC 2328 in 1998 [51]. OSPFv2 was then extended in RFC 2740 to support Internet Protocol version 6 (IPv6) in 1999 as OSPFv3 (or OSPF for IPv6) [52]. Numerous small revisions to the initial RFC have been compiled in an updated version of OSPFv3, RFC 5340 [53].

There have been numerous efforts to develop extensions to OSPF(v2 and v3) that are better suited to wireless environments. These include Radio-OSPF (R-OSPF), a proprietary extension to OSPFv2 developed by BBN Technologies cited in [54], and Wireless OSPF, a proposal made by

Boeing Phantom Works that defines a new type of OSPFv2 interface to limit the number of adjacencies formed between wireless nodes in an attempt to cut down on excessive protocol overhead [55]. Additionally, two competing 'wireless' extensions to OSPFv3, Cisco Systems-developed Overlapping Relays (OR) [56] and the proposal MDR [57] by Richard Ogier, were thoroughly compared through simulation in [58]. The latest revisions of the OR and MDR drafts are [48] and [49] respectively. A third proposal, called the OSPF Multipoint Relay (MPR) extension [50], incorporates the concept of multipoint relaying from the Optimized Link State Routing (OLSR) protocol into the OSPFv3 protocol framework.

The remaining part of this section provides a general overview of OSPFv3 routing protocol operation. Since the simulation and emulation work described in later sections concerns only OSPFv3 and the MDR extension, discussion involving other wireless adaptations of OSPF is omitted. Major literature references for OSPF, excluding RFCs and Internet Drafts, are [59–61].

4.2.1 Overview of OSPFv3

OSPFv3 is a proactive, link-state routing protocol. Routers actively maintain link-state information between all routers in the network and store this information in a link-state database. Changes to one router's link-state database trigger the flooding of an update to the rest of the network along existing links between routers.

Messages

In an OSPFv3 network, routers distribute and collect information to and from each other in order to build routing tables. There are several types of messages that OSPFv3 routers exchange:

- **Hello** - Routers transmit periodic Hello messages in order to inform nearby routers of available links. Routers that exchange Hello messages become *neighbors*.
- **Database Description (DbDesc)** - Once a pair of routers become *neighbors*, they exchange lists of stored routing information (the routers' databases) through DbDesc messages.
- **Link State Request (LSReq)** - While exchanging DbDesc messages, one of the routers may discover that it does not have the same information as its neighbor. A router can request particular information from its neighbors with LSReq messages.
- **Link State Update (LSU)** - As routers learn new information from or about neighbors, they flood this information out over the network in the form of LSUs. LSUs are comprised of

one or more *Link State Advertisements (LSAs)*, containing information on neighboring routers, network address prefixes, protocol configuration values, etc. Several types of LSAs have been defined for OSPFv3 including *Router*, *Network*, *Inter-Area Prefix*, *Intra-Area Prefix*, *Intra-Area Router*, *AS-External*, and *Link* LSAs.

- **Link State Acknowledgement (LSAck)** - LSAck messages acknowledge the receipt of LSUs and help ensure that flooded information reaches the entire network.

Neighbors

As routers discover each other and synchronize databases, each router will associate specific neighbor states to the other connected routers to describe the relationship between them. A few of the important states follow, using the example of two routers, A and B:

- **Down** - Router A is unable to communicate with router B. Router B is considered to be unreachable, or Down, to router A.
- **Two-Way** - Hello messages have been exchanged between routers A and B, meaning bi-directional communication is possible between them. Routers A and B are considered to be Two-Way neighbors of each other. However, neither router participates in the flooding of an LSU sent by the other router.
- **Full** - If routers A and B are Two-Way neighbors, they may synchronize databases with each other, to become Full neighbors, or *adjacent* to one another. LSUs are flooded over adjacencies (links connecting the router to a Full neighbor) only. The procedure to determine whether or not Two-Way neighbors form adjacencies is controlled by the routers' configured interface type.

Interface/Network Types

The interfaces of an OSPFv3 router are assigned specific *interface types* during router configuration. An interface type controls the decision process for forming adjacencies with neighboring routers, as well as the LSU flooding procedure. There are several interface types defined in OSPFv3, which were designed with wired networks in mind. The notion of *network type* comes from the fact that routers on a common link are configured with the same interface type. The relevant interface/network types in OSPFv3 include:

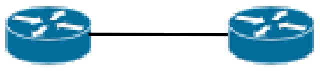

Figure 4.1: Traditional Point-to-Point network consisting of two routers.

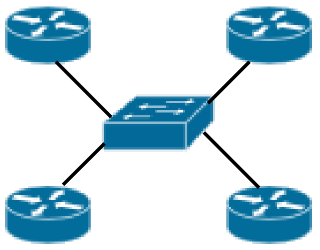

Figure 4.2: Example Broadcast network with four routers and one Ethernet switch.

- **Point-to-Point (PTP)** - A PTP interface is traditionally associated with connecting two routers via a single connection (Figure 4.1). However, PTP interfaces are instructed to use multicast destination addresses for routing control packets. Additionally, neighbor discovery for a PTP interface is dynamic. A PTP interface will begin to keep neighbor state information on other routers as it receives Hello messages from them. Adjacencies in a PTP network are formed between all neighboring router pairs. As a result, it appears possible for a PTP interface to become adjacent to multiple neighbors, and this is seen in OPNET's PTP model (discussed in Section 4.3.2).

- **Broadcast** - A Broadcast interface type can be used when it is known that the network has a 'broadcast capability.' Broadcast capability means that a single packet transmitted over a router's interface to the network has the ability to reach all other routers on the network (e.g., Ethernet, as in Figure 4.2). All routers in a Broadcast network act together in electing a single router as the Designated Router (DR). The elected DR is one-hop communicable with all other devices on the network (due to the broadcast capability of the network). Routers in the network will only form an adjacency with the DR to control the flooding of LSUs. The DR handles Database synchronization and LSU flooding for the entire network. A Backup Designated Router (BDR) is also chosen as a failsafe if the DR should go offline. Broadcast networks are able to take advantage of multicasting routing control packets, and neighbor discovery is also performed dynamically with Hello messages.

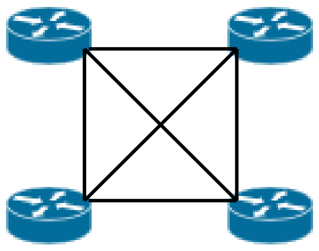

Figure 4.3: Example Non-Broadcast Multiple-Access network showing only logical connections.

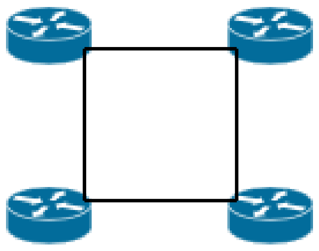

Figure 4.4: Example Point-to-MultiPoint network showing only logical connections.

- **Non-Broadcast Multiple Access (NBMA)** - NBMA networks are similar to Broadcast networks because of the assumption that all routers are logically connected with one another (Figure 4.3). However, NBMA networks do not assume that a broadcast capability exists within the network, such as in Asynchronous Transfer Mode (ATM) or Frame Relay networks. DR election and adjacency formation happens in the same manner as in Broadcast networks, but separate unicast transmissions must be made to each neighbor in order to effectively 'broadcast' packet. Due to the lack of broadcasting, neighbor discovery is not dynamic, and the neighbors of each router are pre-specified during protocol configuration.

- **Point-to-Multipoint (PTMP)** - PTMP networks are considered a type of NBMA network due to the fact that the ability to broadcast does not exist. However, PTMP networks (Figure 4.4) relax the full mesh requirement of NBMA networks and thus are not able to use a DR to control adjacency formation and LSU flooding. Adjacencies are formed between all router pairs in a PTMP network, and separate unicast transmissions are required in order to send a packet to multiple neighbors.

4.2.2 Overview of MDR

As discussed previously, OSPFv2 and OSPFv3 define several types of interfaces including PTP, Broadcast, NBMA, and PTMP interfaces. Broadcast and PTMP fit the requirements for mobile wireless networks the best, but fail in several important ways [55]. Broadcast networks take advantage of multicasting for control messages, but require that the elected DR be one-hop communicable with all other devices on the network. This is not so in a multi-hop environment, and the Broadcast interface proves to be unsuitable for MANETs. A network operating with PTMP interfaces loosens the full mesh requirement of NBMA networks but the original specification assumes that no broadcast capability exists for the communication medium. In a PTMP network, this causes adjacency formation between all communicable routers pairs and quickly saturates the network with protocol overhead traffic [55] due to the inability to multicast control traffic. For example, if PTMP or PTP interfaces were configured on the network shown in Figure 4.5, a single control packet would be flooded out along all links (red, green, and black) by each router in the network, resulting in many redundant transmissions.

The proposed MDR extension to OSPFv3 introduces a new type of interface to cut down on protocol overhead in several ways, namely flooding reduction, adjacency reduction, and topology reduction [62]. The first of these, flooding reduction, involves allowing multihop/partial mesh networks to use Designated Router-like control over flooding by electing a subset of routers in the network as MDRs (Figure 4.5). The MDRs are selected so that they form a backbone that is a Source Independent Connected Dominating Set (SI-CDS) when considering a graph of the network topology. LSU flooding takes place over this backbone. If enabled, Backup MANET Designated Routers (BMDRs) are also chosen so that the backbone is bi-connected. BMDRs only participate in the flooding process if a LSU from an MDR goes unacknowledged. Adjacency reduction is accomplished by restricting the formation of adjacencies to those that are with the (B)MDR backbone. Non-(B)MDR routers are only allowed to form a single adjacency with one MDR (a second adjacency with a (B)MDR is permitted if BMDRs are enabled). Third, topology reduction is achieved by controlling the type and number of routes advertised in LSAs with the parameter *LSAFullness*. *LSAFullness* may take on several values, ranging from minLSA to Full. If set to minLSA, routers only advertise adjacencies, while the Full setting allows routers to advertise all neighbors in state Two-Way or higher.

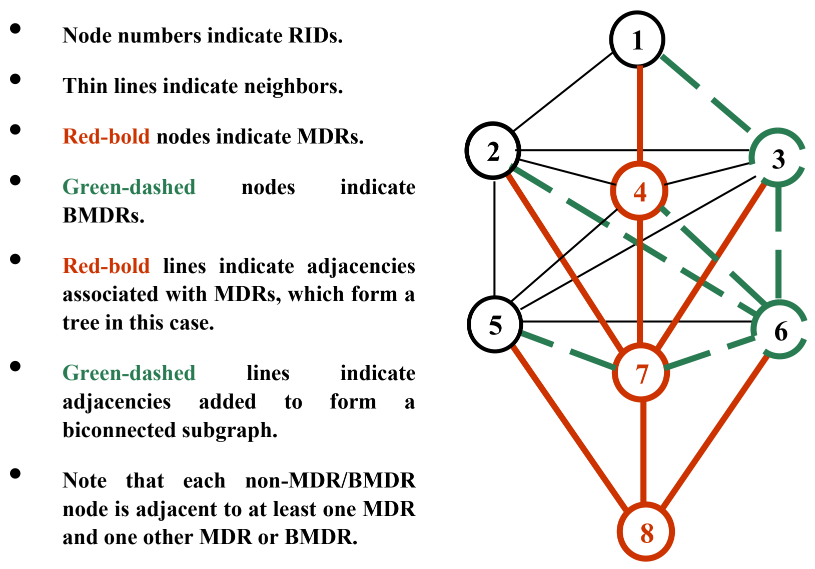

- **Node numbers indicate RIDs.**
- **Thin lines indicate neighbors.**
- **Red-bold nodes indicate MDRs.**
- **Green-dashed nodes indicate BMDRs.**
- **Red-bold lines indicate adjacencies associated with MDRs, which form a tree in this case.**
- **Green-dashed lines indicate adjacencies added to form a biconnected subgraph.**
- **Note that each non-MDR/BMDR node is adjacent to at least one MDR and one other MDR or BMDR.**

Figure 4.5: Example network topology using MANET Designated Routers (adapted from [58]). Note that PTP and PTMP flooding would occur over all links in the network, while MDR flooding occurs only over the red links.

4.3 OSPFv3 Implementation Differences

The performance of OSPFv3 and the MDR extension were measured and compared between an emulation testbed and OPNET simulations. This section introduces the different environments and highlights any known differences between implementations. A brief overview of the emulation testbed is supplied and a more detailed explanation of the OPNET OSPFv3 model implementation is given afterwards.

4.3.1 OSPFv3 in Emulation Testbed

The emulation testbed consisted of several racks of Linux-based PCs interconnected through an Ethernet switch with high-speed, Gbps links. The PCs were configured as Linux OSPFv3 routers using the Quagga routing suite [63]. Links between routers were managed by creating Virtual Local Area Networks (VLANs) between router pairs and enabling or disabling them as necessary in order to emulate the dynamic nature of wireless links in a MANET, as discussed later in Section 4.4.1.

The version of Quagga used in the emulation testbed matches that of a Boeing Phantom Works study [58]. The primary purpose of the Boeing study was to evaluate competing proposals (MDR and OR) for a new wireless interface type for OSPFv3. Quagga was patched to include support for both the OR and MDR extensions. It was found that the OSPFv3 implementation in this Quagga package (including the Boeing patches) included multicast support for PTMP interfaces. The MDR extension implementation was cited by [58] to be generally consistent with the 4th version of the Internet Draft [57]. More information can be found in [55,58,62]. For a thorough explanation of the emulation testbed setup and management, refer to [7].

4.3.2 OSPFv3 in OPNET

Simulations were performed using OPNET Modeler 12.0 PL5 on a Linux platform running the Redhat Enterprise Linux WS release 4 (Nahant Update 5) operating system. For reasons explained later in this section, a custom patch was needed for OPNET's OSPFv3 PTP interface. There were many resources that were used to become more familiar with the OPNET implementation of OSPFv2, OSPFv3, and the MDR extension, including OPNET Documentation, FAQ's, and [51,52,59–61,64]

Interface/Network Types

The standard interface types in OPNET generally operate in the manner described in Section 4.2.1. However, OPNET's MANET interface for OSPFv3 is a partial implementation of Ogier and Spagnolo's MDR proposal [64]. The following are specifics on the behavior and usage of the standard OPNET OSPFv3 interface types and the differences between the OPNET MANET interface and the MDR specification that were found.

- **OPNET PTMP Interface** - According to the RFCs [51,52], OPNET's OSPFv3 PTMP interface sends all routing protocol messages (including Hello, Link-State Update, and Link-State Acknowledgements) as unicast transmissions over each router-to-router adjacency. Furthermore, neighbor discovery is not dynamic, and neighboring routers must be supplied during configuration of each router in the PTMP network. This has two major implications for simulations using this type of OSPFv3 interface.

  First, an OSPFv3 router will not discover its neighbors dynamically. Each neighbor's global IPv6 address must be specified prior to simulation. Each router will use its list of neighbors when sending Hello messages over its PTMP interface. A copy of the message is unicast to each neighbor in the list.

  Furthermore, simulation of a *mobile* wireless network requires that each router's neighbor list contain the set of all other routers it will form adjacencies with over the course of the simulation, not just the routers that are initially within communication range. If the mobility patterns are not known ahead of time, these sets of neighbors cannot be predicted, and it becomes necessary to assign each router's neighbor list to the set of all other routers in the network. However, this will cause a unicast Hello message to be sent to every other router in the network, even though a small fraction of them may actually be neighbors at a given time instant. LSUs and LSAcks are also sent as unicast transmissions along each adjacency.

- **OPNET PTP Interface** - According to the RFCs, [51,52], OPNET's OSPFv3 PTP interface sends the majority of routing protocol messages as multicast packets. The OPNET interface type also supports dynamic neighbor discovery, meaning pre-specification of neighbors is not necessary. If OPNET is used as a validation tool for the PTMP results obtained with the patched Quagga package from the Boeing Phantom Works study, *it is recommended that the OPNET OSPFv3 PTP interface be directly compared to the Boeing-enhanced Quagga OSPFv3 PTMP interface.*

- **OPNET MANET/MDR Interface** - The OPNET OSPFv3 MANET interface implementation was designed according to the 6th version of the MDR Internet Draft [64]. However, as mentioned in the OPNET Model Documentation (for Modeler 12.1 PL0) there are certain features of the Internet Draft that are not implemented in OPNET. It is possible to enable the selection of BMDRs in OPNET, which should strengthen the LSU flooding backbone, but the ability of BMDRs to retransmit unacknowledged LSUs is not present in the standard OPNET OSPFv3 model. The *LSAFullness* parameter has several values specified in the Internet Draft to control the number of routers advertised in LSUs. These include minLSA, mincostLSA, and MDRFullLSA. The OPNET implementation currently supports the minLSA option only. When validating the emulation testbed using OPNET, it is important to make sure that the emulation testbed OSPFv3 settings are configured so that an equivalent environment in OPNET can be set up.

LSA Origination & Generation

During experimentation and simulation (described more fully in Section 4.4), it was discovered that OPNET's implementation of OSPFv3 was generating more overhead than the patched Quagga routing package running on the emulation testbed. Discussion with OPNET Tech Support led to the determination that Link LSAs and Intra-Area Prefix LSAs were being advertised in LSUs every

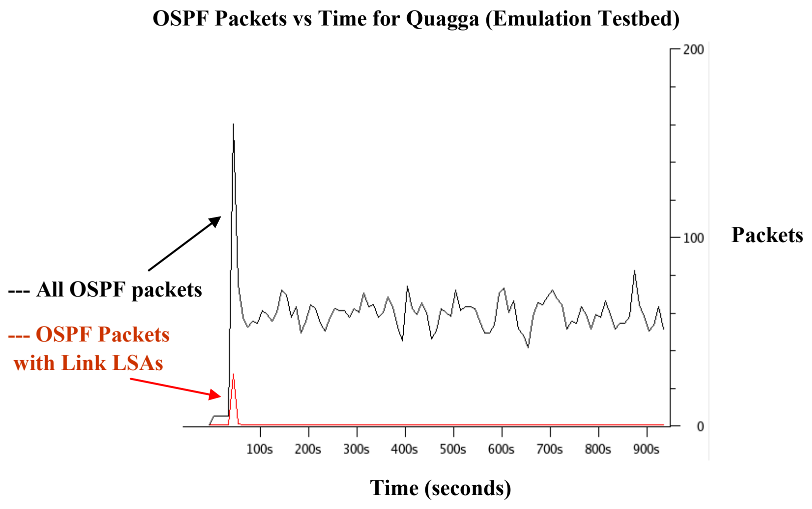

Figure 4.6: Link LSA suppression in emulation testbed, generated from Wireshark packet trace.

time an adjacency in the network was broken or formed for OPNET PTP interfaces. Link LSAs and Intra-Area Prefix LSAs help propagate prefix and protocol configuration information throughput the network and do not affect the way routes are calculated in OSPFv3. They are generally flooded throughout the network as routers begin protocol operation and can be suppressed after initial origination. Investigation of the emulation testbed's OSPFv3 log files and Wireshark [65] packet capture traces confirmed that Link-LSAs and Intra-Area Prefix LSAs were not transmitted in the network beyond protocol startup of the patched Quagga OSPFv3 package. In particular, Figure 4.6 shows the Link-LSA suppression in the emulation testbed by displaying the amounts of control packets generated over the duration of an emulation testbed experiment involving 30 routers. The amount of packets with Link LSAs quickly die off after the beginning of the experiment. A patch was issued by OPNET Tech Support to suppress the redundant LSA origination for OPNET PTP interfaces.

OPNET OSPFv3 Parameters

Many OSPFv3 parameters in OPNET are configurable as model attributes. However, there were several OSPFv3 parameters that were either not available for modification or were unused.

The *LS_Refresh_Time* parameter forces routers to re-originate LSAs whose ages exceed the parameter's value. The default for this parameter is 30 minutes. The parameter is defined in the OPNET OSPFv3 model code, but is not referenced elsewhere. As a result, simulations lasting longer than 30 minutes would not include the LSU flooding associated with refreshing older LSAs (according to the parameter *LS_Refresh_Time*).

The *MinLSArrival* parameter is the maximum rate that routers accept updates for any particular LSA [59]. In OPNET, this value is fixed to once every 1 second. The *MinLSInterval* parameter is the maximum rate that routers will update any particular LSA [59]. OPNET set this value to once every 5 seconds. These parameters attempt to reduce overhead during turbulent network conditions that cause frequent LSA changes.

The ability to delay the flooding of LSAs is present in the OPNET MANET interface and was enabled for the PTP interface by the OPNET Modeler patch (mentioned in Section 4.3.2). This is known as coalescing of LSAs and is a measure taken to save overhead, by holding back the initial flooding of LSAs until more LSAs can be packaged into an LSU and sent out together. However, the method does introduce some amount of delay into the affected packets. Both the MANET and PTP interfaces in OPNET delay the generation of Router LSAs by 1 second. Finally, the ability to delay and coalesce LSAck messages is present in both the PTP and MANET interfaces in OPNET. For MANET interfaces, LSAck messages can be delayed by at most 1 second, while PTP interfaces can delay acknowledgements up to 1/2 the value of the retransmission interval. A typical value for the retransmission timer is 5 seconds.

4.4 Creating Equivalent Scenarios

The OPNET scenarios used to validate the emulation testbed were constructed iteratively as both the simulation and emulation environments were changed and tweaked to match each other. Experiments on the emulation testbed were conducted for 10 through 30 routers in increments of 5. Overall, scenario construction in OPNET was performed in the same manner for each network size tested. The issues and challenges involved in establishing equivalent simulation environments for both tasks are detailed here.

4.4.1 Mobility Matching

Since the emulation testbed consisted of wired routers, a method of emulating node movement needed to be devised. Devices in a MANET are primarily aware of node mobility only through changes to the network topology. As nodes move toward and away from each other, the ‘links’ between them go up or down correspondingly. To achieve realistic topology changes in the emulation testbed, traces of node mobility patterns were recorded in OPNET and fed into the emulation testbed. The information in the traces included node positions and link changes, which listed time, node pair, and link status change (up, down) at a granularity of 1 second intervals. The link between nodes was considered 'up' if the distance separating them was less than or equal to 250 meters. Note that the link information passed to the emulation testbed did not include interference levels, as the emulation testbed did not yet contain functionality for modeling interference.

Each constructed simulation scenario had dimensions of 500 meters by 500 meters. OPNET mobile nodes of type *wlan_ethernet_router_adv* were placed in the scenario in the required amounts (10, 15, 20, 25, 30 routers). Furthermore, nodes were configured to move according to a Random Waypoint (RWP) mobility model [23] with a constant speed of 20 m/s and pause times of 40 seconds. Snapshots of network connectivity were withheld until 1800 seconds into the simulation so that the RWP model could approach steady-state [66] before mobility traces were provided to the emulation testbed.

4.4.2 Channel Model Matching

The emulation testbed required some compromise from the simulation environment concerning the physical channel. Routers in the emulation testbed were connected to an Ethernet switch with 1 Gbps links. Transmission delay, propagation delay, and collisions were effectively negligible in the emulation environment. However, the MANET in the OPNET scenarios consisted of wireless Institute of Electrical and Electronics Engineers (IEEE) 802.11b routers. As a result, propagation and transmission delays as well as collisions and retransmissions became significant factors in the operation of higher layer functions like routing. Functionality to emulate these lower layer effects was not yet implemented in the emulation testbed, so a second, simpler channel model was used in the simulation testbed in addition to the standard channel model associated with IEEE 802.11b radio.

- **Standard OPNET Radio Pipeline -** The standard OPNET radio pipeline stages compute received power, interference, Signal to Interference and Noise Ratio (SINR), Bit Error Rate (BER), bit errors, and error correction. Only a few physical layer parameters were changed from the defaults set in the *wlan_ethernet_router_adv* node model. Using the Friis transmission equation [67] present in the standard radio pipeline stage *wlan_power.ps.c*, it was determined that, in freespace conditions, a signal transmitted at ~ 0.25 Watts would be received with a signal strength of -64 dBm at a distance of 250 meters away from the source. Antenna gains were assumed to be at a default of 0 dB and the transmitted wavelength was calculated from the center frequency of the first IEEE 802.11b channel. As a result, the transmit power was changed to 0.25 Watts and the receiver threshold was set to -64 dBm, so that nodes could still communicate at up to a maximum of 250 meters away from each other.

- **Distance-based Radio Pipeline -** The distance-based channel model set all of the standard radio pipeline stages to NONE except for the power, rxgroup, closure, and chanmatch stages. Packet reception was effectively evaluated using the distance separating the transmitter and receiver (using the Friis transmission equation [67]), and packet deliveries were performed without delay. Later stages, such as interference, SINR, and BER were ignored. These changes to the channel model amounted to another step towards more equivalent scenario representation between the simulation and emulation environments. While simplifying the OPNET channel model to match the emulation testbed is admittedly worse from a model fidelity point of view, the procedure was carried out because it is considerably easier to change OPNET models than to modify the emulation testbed medium access and physical layers. The modifications of the channel model in OPNET were a sufficient first pass at closing the differences between the simulation and emulation data link layers, until more advanced emulation features could be introduced to the testbed.

4.4.3 Network Layer Matching

Experiments on the emulation testbed were conducted for both the modified PTMP and MANET/MDR interfaces of the patched Quagga OSPFv3. Separate OPNET simulations were conducted with PTP and PTMP interfaces, both for comparison with the patched Quagga PTMP. Additionally, simulations with OPNET's MANET interface were compared directly with the patched Quagga MDR implementation. Most configuration details remained the same regardless of the interface type in OPNET. OPNET parameters that differ from their default values are listed in Table 4.1.

Additionally, when configuring a PTMP interface in OPNET, each router must be supplied with a list of neighboring routers, as discussed in Section 4.3.2. Regarding the MANET parameters, differential Hello messaging and BMDRs were disabled (BMDR flooding is not implemented as mentioned previously).

Table 4.1: OSPFv3 Routing Parameters

Parameter Name	Value
Start Time	uniform(1800.0,1810.0)
SPF Calculation Parameters	LSA Driven
Hello Interval (seconds)	2
Router Dead Interval (seconds)	6
Retransmission Interval (seconds)	5
Full Hello Frequency	Every First
Hello Repeat Count	Once
Adjacency Connectivity	Uniconnected

4.5 Simulation/Emulation Results Comparison

Validation of the emulation testbed took several iterations of simulations. As more was learned about the simulation environment and the OPNET implementation of OSPFv3 and the MDR extension to OSPFv3, changes and updates to the simulation environment were made to match the emulation testbed. The following results detail the incremental updates to the simulation environment and show the difference between performance curves of the two environments at each step.

4.5.1 PTMP vs PTP interfaces in OPNET

Behaviorally, the PTMP interface in OPNET was not the same as the PTMP emulation interface. It was determined that OPNET's PTMP interface was initiating packet transmissions according to the OSPFv3 IETF RFC. Following the specification, each router in OPNET sent Hello messages as separate unicast transmissions to each of their neighbors and sent LSAck and LSU packets as unicast transmissions along each of their adjacencies. However, the emulation testbed's OSPFv3 PTMP interface was modified beyond the specification to support the multicasting of routing control packets to take advantage of a broadcast (wireless) environment (and thus decrease unnecessary overhead).

Unlike the OPNET PTMP interface, the PTP interface in OPNET supported multicasting and was deemed a much closer match to the emulation testbed in terms of protocol behavior. To compare the two interface types, OPNET simulations were performed with both the PTMP and PTP interfaces using the *wlan_ethernet_router_adv* node model (standard radio pipeline stages) with network sizes of 10 to 40 routers. The measured overhead from each of these combinations is shown in Figure 4.7 and is compared with the measured overhead from the emulation testbed. The benefits of multicasting are apparent in the OPNET PTP performance curve, as there is decreased overhead

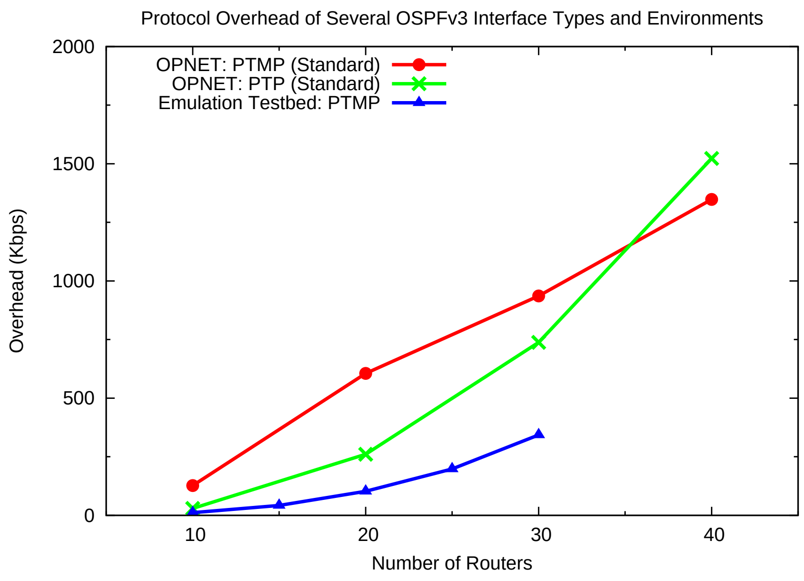

Figure 4.7: Overhead differences between OPNET PTP and PTMP interfaces.

compared to the OPNET PTMP performance curve. Additionally, the OPNET PTP interface produced overhead measurements that were closer to those reported by the emulation testbed. As a result, further simulations in the study were conducted with OPNET's PTP interface.

4.5.2 Radio Pipeline Stages

Since the emulation testbed's Ethernet medium access and physical layers were much different than those of the IEEE 802.11b standard, an alternate set of radio pipeline stages were configured. The new set of stages eliminated any propagation or transmission delay and evaluated the successful reception of packets based only on distance. Simulations for both the standard radio pipeline stages and the distance-based radio pipeline stages were conducted for network sizes of 10 to 40 routers. The measured overhead and packet generation rates for all simulations runs are plotted in Figure 4.8 and Figure 4.9 respectively and compared with emulation testbed measurements. In the debugging logs generated by the emulation testbed, the distinction between multicast (M) and unicast (U) packets was not made. Both categories (M) and (U) were grouped under the appropriate multicast columns in the figures.

In general, the amount of overhead and packet generation rates decrease once the simplified radio pipeline stages are substituted into OPNET simulations. The distance-based packet reception model and zero delay packet delivery virtually eliminate contention for the media and packet loss. Note

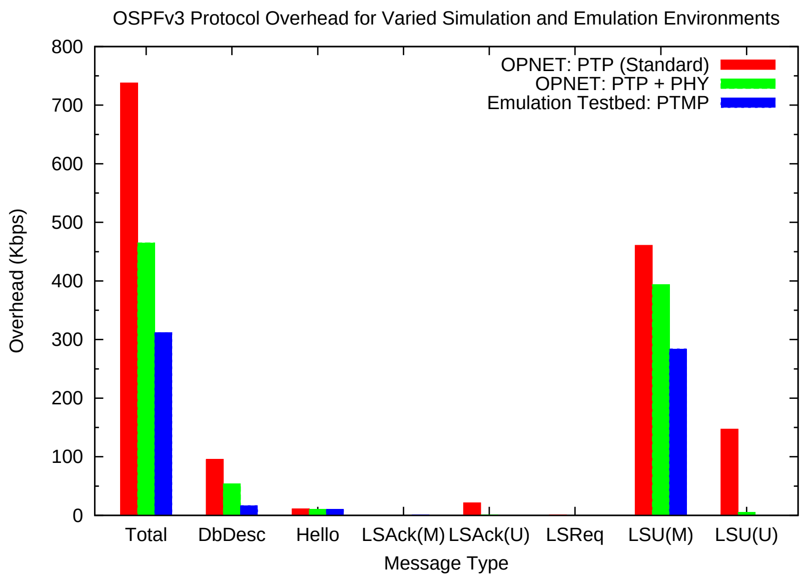

Figure 4.8: Overhead differences between OPNET radio pipeline stage configurations.

that packet loss is still possible if nodes initiate a transmission attempt while out of communication range. The biggest drop in overhead and packet rates comes from unicast LSU messages. From the OSPFv2 specification [51], Section 8.1 states that retransmissions of LSU messages are always sent as unicast transmissions. It is highly likely that the simplified physical layer model, which nearly eliminates collisions and dropped packets, is reducing the number of packet retransmissions. This correlates with the severe drop in unicast LSUs transmissions. Overall, the reported overhead and packet rates for OPNET PTP move closer to that reported by the emulation testbed.

Results in Figure 4.8 and Figure 4.9 are only shown for the OPNET PTP interface and the emulation testbed's PTMP interface. The overhead and packet generation rate trends for the MANET (MDR) interface were very similar between the simulation and emulation environments and less demonstrative. The MANET (MDR) interface is specifically designed to produce less routing traffic than the PTP interface in a wireless environment and demands less of the channel, resulting in a smaller, but similar, effect when simplifying the pipeline stages.

4.5.3 Results Summary

Final results involving OPNET's MANET (MDR) interface are shown in Figure 4.10 and Figure 4.11 and contain the overhead and packet generation rates along with equivalent emulation testbed measurements. The displayed OPNET measurements were taken from simulations that applied the

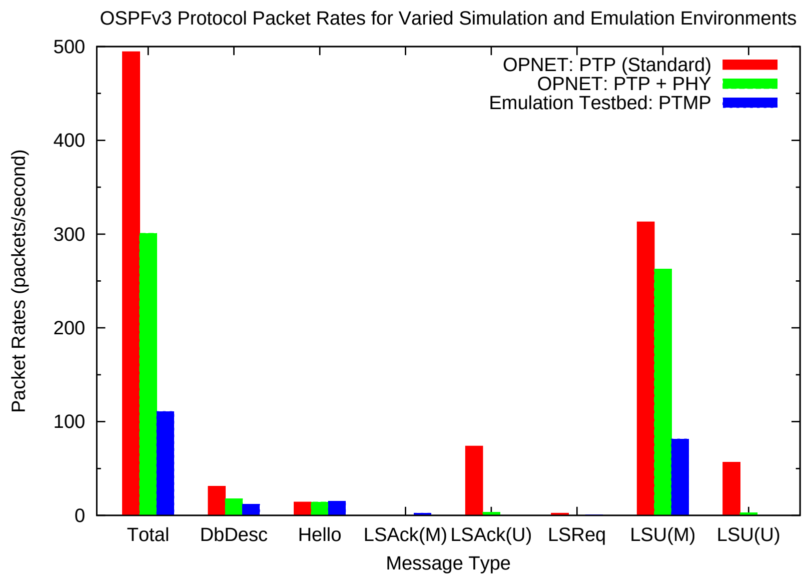

Figure 4.9: Packet generation rate differences between OPNET radio pipeline stage configurations.

distance-based radio pipeline stages for a network size of 30 routers. In the results gathered from the emulation testbed, the distinction between multicast (M) and unicast (U) packets was not made, and both were grouped under the appropriate multicast columns in both figures.

The packet rates in OPNET and the emulation testbed in Figure 4.11 were very close for all packet types recorded. However, the overhead reported in Figure 4.10 for both environments differed to some degree. This difference made itself apparent in the overhead associated with LSU messages sent in both environments. Clearly, similar numbers of LSU packets were being generated in each environment, but the emulation testbed appears to be packing more information in each packet. The exact cause of this difference is unknown at this time, but further investigation should be directed towards examining the types of LSAs contained within the LSU messages.

Figure 4.12 shows the overhead recorded for all OSPFv3 interfaces, simulated and emulated, for network sizes ranging from 10 to 40 routers. In particular, it can be seen how the OPNET simulations approach the reported overhead of the emulation testbed as each change to the simulation environment was made. These changes include switching focus from the OPNET PTMP interface to the OPNET PTP interface because the latter behaved more closely to the emulation testbed in terms of multicasting and dynamic neighbor discovery. Next, the distance-based radio pipeline stages were substituted into the OPNET simulations (indicated by the curve labeled OPNET: PTP + PHY) and another drop in reported OSPFv3 overhead occurred due to the nearly eliminated

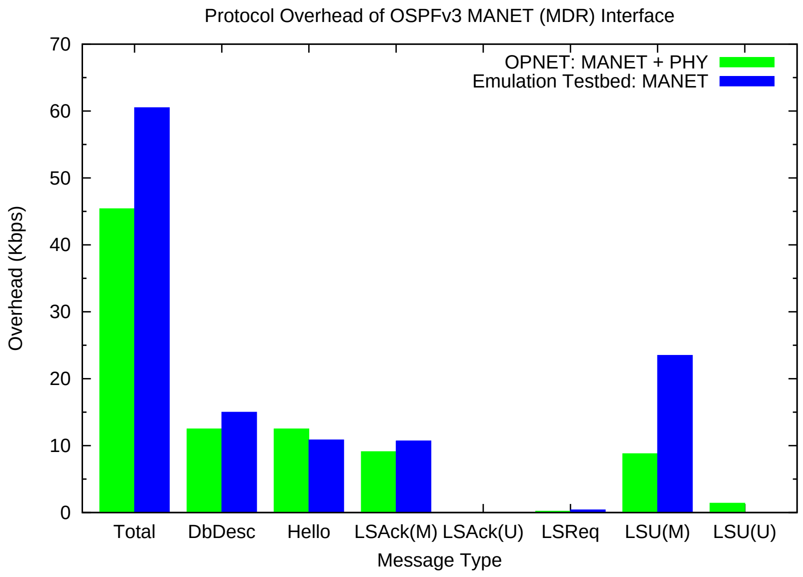

Figure 4.10: Overhead differences between OPNET and emulation testbed MANET (MDR) interface.

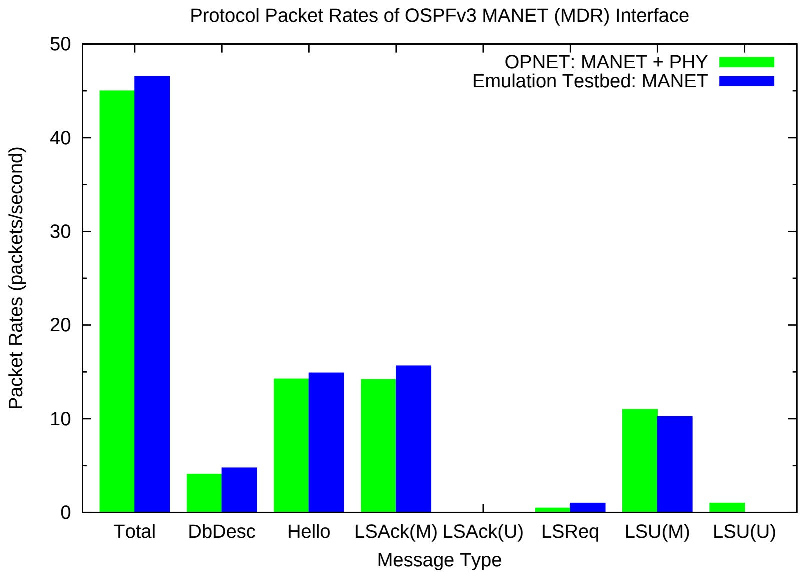

Figure 4.11: Packet generation rate differences between OPNET and emulation testbed MANET (MDR) interface.

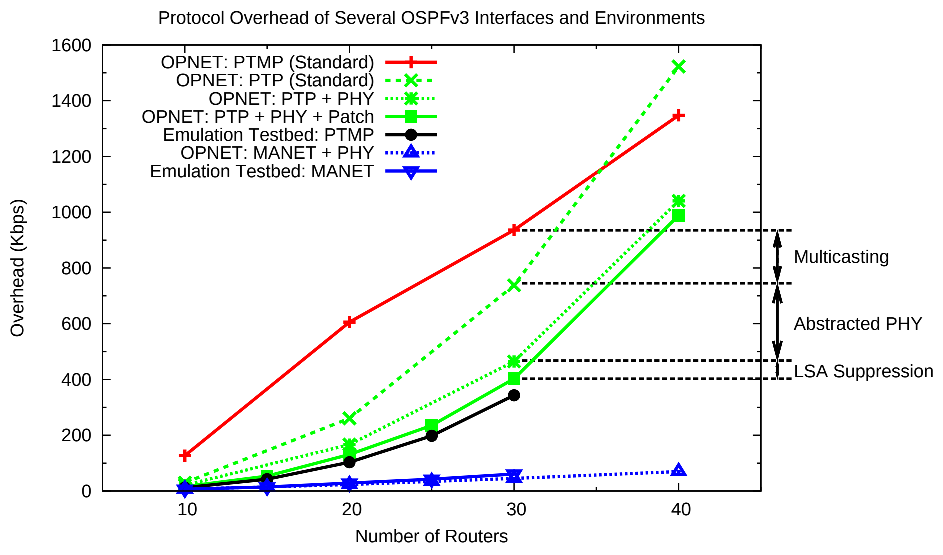

Figure 4.12: OSPFv3 overhead reported for several simulation and emulation environment configurations.

packet collisions and drops. Finally, the OPNET patch discussed in Section 4.3.2 was applied to the PTP simulations (indicated by the curve OPNET: PTP + PHY + PATCH) and further reduced the OSPFv3 overhead. Due to the relatively small changes in the MANET (MDR) interface results, only the final simulation configuration is compared with the emulation testbed.

Table 4.2 lists the percent errors of the final PTP and MANET simulation environments relative to the emulation environment for each common network size tested. From the table, it can be seen that the percent error of the OPNET PTP simulations decreases as the network size increases. In direct contrast, the OPNET MANET simulations show increased percent error as the network size grows. If the percent error for either interface type were constant over the difference network sizes, that fact would help establish the ability to predict the overhead generated by the emulation environment given the data from OPNET simulation (or vice versa). This is useful for cases where the simulation environment has the ability to scale to network sizes beyond the existing capabilities of the emulation environment (Figure 4.13). However, neither percent error trend is constant, which suggests there is additional work needed to resolve remaining differences between the two environments.

Table 4.2: OPNET Percent Error Relative to Emulation Testbed Measurements

Network Size (routers)	**OPNET PTP+PHY+PATCH % Error**	**OPNET MANET(MDR)+PHY % Error**
10	31.33	4.80
15	25.56	1.70
20	27.02	18.90
25	18.80	18.12
30	17.30	26.18
$\% \text{ Error} = \lvert\text{Observed} - \text{Actual}\rvert/\text{Actual} * 100 = \lvert\text{OPNET} - \text{Emulation}\rvert/\text{Emulation} * 100$		

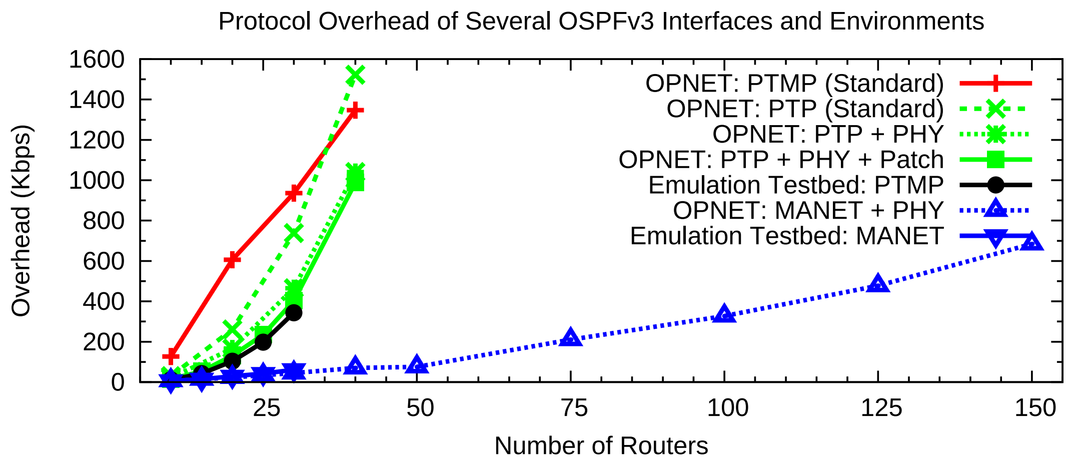

Figure 4.13: Scaling to larger networks with simulation.

4.6 Conclusions

The study detailed in this chapter and [7] represents an initial step in the use of simulation and an emulation testbed to cross-validate the performance of a proposed wireless extension to the OSPFv3 routing protocol. Two independent representations of the same protocol specifications (OSPFv3 and the MDR extension) were studied; a behavioral model in the OPNET simulation environment and actual routing software in an emulation testbed.

Research on OSPFv3 through previous studies and protocol specifications was conducted to gain a better understanding of the performance benefits offered by the MDR extension to OSPFv3 and to formulate expectations on the performance of the different OSPFv3 interface types in the behavioral models and routing code. This research revealed differences between the two environments, such as the multicasting-enabled PTMP interface in the patched-Quagga routing suite.

Simulation and experimentation yielded further implementation and environment dissimilarities that were causing performance differences. It was found that the OPNET implementation of OSPFv3, unlike the patch-Quagga OSPFv3, was not suppressing particular LSAs. A patch was introduced to correct this and performance differences decreased. Additionally, measures were needed to match the simulation and emulation environment, such as equivalent mobility modeling and similar physical and data link layer representations. These changes, while not involving OSPFv3, were also key in closing performance gaps.

Overall, the validation effort stresses the importance of verifying protocol specifications and operation through the use of multiple independent sources. By consulting many sources, some confidence was established that the protocol is working as intended, and it revealed implementation assumptions and differences in OPNET that would have otherwise gone unnoticed.

4.7 Future Work

There are several topics that could continue this line of work. Within the scope of the emulation testbed, it is perhaps most important to refine the channel model in the emulation testbed. Incorporating interference and transmission delays into the emulated channel would offer more realistic estimates of network performance.

Furthermore, it would be helpful to refine statistics collection for both environments. The ability to report separate categories for multicast and unicast packets such as LSU and LSAck messages in the emulation testbed would be useful for further comparison. Additionally, the ability to investigate the type and amount of specific types of LSAs being packaged into LSUs would be very helpful in continuing the investigation of remaining differences between the emulation and simulation environments.

If the MANET (MDR) extension of OSPFv3 is to be studied further, it would be useful to have more *LSAFullness* options and BMDR flooding built into the OPNET implementation. In this study, testing of the MANET interface was rather limited due to the lack of options in OPNET's implementation.

Finally, ways to extend this study include modeling application traffic on top of the routing protocol. This would open the ability to study performance metrics such as packet delivery percentage and packet latency among others. Another important branch from this study includes modeling and emulating the other proposed OSPFv3 wireless extensions.

5. Conclusions

This body of work presented three case studies that a.) highlight issues affecting the use of simulation as well as b) detail ways of applying simulation to the study of wireless networking protocols.

The performance of simulators, measured in both accuracy of results and run time, is a constant concern to simulation users. Chapter 2 developed three abstractions of the IEEE 802.11 RTS/CTS channel access mechanism in order to combat prohibitively high running times in simulations of large scale mobile ad hoc networks. The design of the abstractions sought to decrease scaling of simulation runtime with network size by combining events and reducing the number of receivers considered for physical layer calculations for control frames. Each level of abstraction did manage to improve on the run time required to complete a simulation. In particular, the 'best' abstraction was the Simplified Neighbor List which achieved near-linear scaling.

Simulations of the abstracted models yielded goodput results that were very comparable to those of the OPNET validation model, but contained some discrepancy in the data trends for ETE delay measurements. This discrepancy is likely rooted in the fact that all three abstractions compressed RTS and CTS events together into an instantaneous transmission, which would have a direct effect on time-based metrics such as ETE delay. Future work with RTS/CTS abstraction includes studying additional abstraction methods to developing the notion that different forms of protocol abstraction are best suited for collecting particular data. Such a study would attempt to yield guidelines in choosing the best abstraction model given a desired metric.

Chapter 3 examined the feasibility of a new protocol via simulation, before involving the costs of any testbed hardware. A literature survey of autoconfiguration schemes designed for MANETs was provided, with particular focus on a stateless autoconfiguration scheme by Jelger and Noel (SECON 2005). The selected scheme provides globally routable IPv6 prefixes to a MANET attached to the Internet via gateways. Initially, the OPNET protocol model was validated against the original authors' data to ensure proper operation. Discussion with the J&N protocol authors revealed simulation setup differences as potential sources for differences in prefix hold times in the validation scenario.

The Jelger-Noel scheme was also examined with new cluster mobility models, added gateway mobility, and varied network sizes. Performance of the Jelger-Noel scheme, derived from overhead, autoconfiguration time and prefix stability metrics, was found to be highly dependent on network density. Low prefix hold time measurements were noted, and it was suggested that ad hoc nodes may experience difficulties in maintaining higher layer sessions. The J&N protocol may need be revised further to improve performance in this area. Areas of future work include investigating potential tradeoffs between prefix hold times and percentage of time without a prefix, controlled by network density.

Finally, in Chapter 4, simulations cross-validated an emulation testbed running the Open Shortest Path First (OSPF) routing protocol and its MANET Designated Router (MDR) extension. Protocol specifications and previous OSPF studies were researched to gain a better understanding of the performance benefits offered by the MDR extension to OSPFv3, and to develop performance expectations in both the simulator's behavioral code and the emulation testbed's protocol implementation. This research revealed differences between the two environments, such as the multicasting-enabled PTMP interface in the patched-Quagga routing suite. The measured OSPF overhead and packet rates from both environments was used as a benchmark to construct equivalent MANET representations and protocol configuration, made particularly challenging due to the wired nature of the emulation testbed.

During the process of performance matching, simulation and experimentation yielded further implementation and environment dissimilarities that were causing performance differences. It was found that the OPNET implementation of OSPFv3, unlike the patch-Quagga OSPFv3, was not suppressing particular LSAs. A patch was introduced to OPNET to correct this and performance differences decreased. Additionally, measures were needed to match the simulation and emulation environment, such as equivalent mobility modeling and similar physical and data link layer representations. These changes, while not involving OSPFv3, were also key in closing performance gaps. Overall, both validation efforts in the study stressed the importance of verifying protocol specifications and operation through the use of multiple independent sources. By cross-validating simulation and emulation data, the simulation's OSPF model limitations were revealed, and confidence was established that the protocol is configured and working as intended in the emulation testbed.

Bibliography

[1] L. Breslau, D. Estrin, K. Fall, S. Floyd, J. Heidemann, A. Helmy, P. Huang, S. McCanne, K. Varadhan, Y. Xu, and H. Yu, "Advances in network simulation," *IEEE Computer*, vol. 33, pp. 59–67, May 2000.

[2] B. Blum, T. He, and Y. Pointurier, "MAC layer abstraction for simulation scalability improvements." Computer Science Department, University of Virginia, December 2001.

[3] P. Zheng and L. M. Ni, "Empower: A scalable framework for network emulation," in *Proceedings of the 31th Annual IEEE International Conference on Parallel Processing (ICPP '02)*, pp. 185–192, August 2002. Vancouver, British Columbia, Canada.

[4] J. Wildman, B. Willman, M. Kirkpatrick, and S. Weber, "RTS/CTS data link abstractions for mobile ad hoc networks," in *Proceedings of the 25th Annual IEEE Military Communications Conference (MILCOM '06)*, October 2006. Washington, DC, USA.

[5] C. Jelger and T. Noel, "Proactive address autoconfiguration and prefix continuity in IPv6 hybrid ad hoc networks," in *Proceedings of the 2nd Annual IEEE Sensor and Ad Hoc Communications and Networks Conference (SECON '05)*, pp. 107–117, September 2005. Santa Clara, CA, USA.

[6] J. Wildman, D. Hamel, R. Measel, D. Oakum, S. Weber, and M. Kam, "Performance and scaling of wireless ad hoc IPv6 stateless address autoconfiguration under mobile gateways," in *Proceedings of the 26th Annual IEEE Military Communications Conference (MILCOM '07)*, October 2007. Orlando, FL, USA.

[7] G. Carl, S. Dastangoo, and J. Wildman, "Using an emulation testbed to measure OSPF routing overhead due to mobility in wireless ad hoc networks," in *Proceedings of the 27th Annual IEEE Military Communications Conference (MILCOM '08)*, November 2008. San Diego, CA, USA.

[8] V. Naoumov and T. Gross, "Simulation of large ad hoc networks," in *Proceedings of the 6th Annual ACM International Workshop on Modeling Analysis and Simulation of Wireless and Mobile Systems (MSWiM '03)*, pp. 50–57, September 2003. San Diego, CA, USA.

[9] "OPNET modeler." Online: `http://www.opnet.com/`.

[10] X. J. Liu, *Improvements in Conservative Parallel Simulation of Large-scale Models*. PhD thesis, Dartmouth College, Hanover, NH, USA, February 2003.

[11] C. Liu, M. A. Orgun, and K. Zhang, "A parallel execution model for Chronolog," *International Journal of Computer Systems Science and Engineering*, vol. 16, no. 4, 2001.

[12] M. Takai, R. Bagrodia, A. Lee, and M. Gerla, "Impact of channel models on simulation of large scale wireless networks," in *Proceedings of the 2nd Annual ACM International Workshop on Modeling Analysis and Simulation of Wireless and Mobile Systems (MSWiM '99)*, pp. 7–14, 1999.

[13] T. He, B. Blum, Y. Pointurier, C. Lu, J. A. Stankovic, and S. Son, "MAC layer abstraction for simulation scalability improvements in large-scale sensor networks," in *Proceedings of the 3rd Annual International Conference on Networked Sensing Systems (INSS '06)*, Transducer Research Foundation (TRF), May 2006. Chicago, IL, USA.

[14] J. Heidemann, N. Bulusu, J. Elson, C. Intanagonwiwat, K. Lan, Y. Xu, W. Ye, D. Estrin, and R. Govindan, "Effects of detail in wireless network simulation," in *Proceedings of the SCS Multiconference on Distributed Simulation*, pp. 3–11, Society for Computer Simulation (SCS), January 2001.

[15] M. Takai, J. Martin, and R. Bagrodia, "Effects of wireless physical layer modeling in mobile ad hoc networks," in *Proceedings of the 2nd Annual ACM International Symposium on Mobile Ad Hoc Networking and Computing (MobiHoc '01)*, pp. 87–94, October 2001. Long Beach, CA, USA.

[16] M. Pidd, "Five simple principles of modelling," in *Proceedings of the 1996 Winter Simulation Conference (WSC '96)*, pp. 721–728, December 1996. Coronado, CA, USA.

[17] D. D. Cavin, Y. Sasson, and A. Schiper, "On the accuracy of MANET simulators," in *Proceedings of the 2nd Annual ACM Workshop on Principles of Mobile Computing (POMC'02)*, pp. 38–43, October 2002. Toulouse, France.

[18] L. F. Perrone and D. M. Nicol, "Using n-body algorithms for interference computation in wireless cellular simulations," in *Proceedings of the 8th Annual IEEE International Symposium on Modeling, Analysis and Simulation of Computer and Telecommunication Systems (MASCOTS '00)*, pp. 49–56, August 2000. San Francisco, CA, USA.

[19] J. Liu, D. M. Nicol, L. F. Perrone, and M. Liljenstam, "Towards high performance modeling of the 802.11 wireless protocol," in *Proceedings of the 2001 Winter Simulation Conference (WSC '01)*, vol. 2, pp. 1315–1320, December 2001. Arlington, VA, USA.

[20] L. C. Zhong and J. M. Rabaey, "Modeling and analysis of the data link layer in wireless sensor networks." Berkeley Wireless Research Center, Department of EECS, University of California at Berkeley. Online: `http://bwrc.eecs.berkeley.edu/People/Grad_Students/czhong/restricted/ICC2003.pdf`.

[21] N. Golmie, R. E. Van Dyck, and A. Soltanian, "Interference of Bluetooth and IEEE 802.11: Simulation modeling and performance evaluation," in *Proceedings of the 4th Annual ACM International Workshop on Modeling, Analysis and Simulation of Wireless and Mobile Systems (MSWiM '01)*, pp. 11–18, July 2001. Rome, Italy.

[22] A. Heindl and R. German, "Performance modeling of IEEE 802.11 wireless LANs with stochastic Petri nets," *Performance Evaluation*, vol. 44, pp. 139–164, April 2001.

[23] T. Camp, J. Boleng, and V. Davies, "A survey of mobility models for ad hoc network research," *Wireless Communications and Mobile Computing*, vol. 2, no. 5, pp. 483–502, 2002.

[24] J. Yoon, M. Liu, and B. Noble, "Random waypoint considered harmful," in *Proceedings of the 22nd Annual IEEE Conference on Computer Communications (INFOCOM '03)*, vol. 2, pp. 1312–1321, March 2003. San Francisco, CA, USA.

[25] C. S. R. Murthy and B. S. Manoj, *Ad Hoc Wireless Networks: Architectures and Protocols.* Prentice Hall Professional Technical Reference, 2004.

[26] "Part 11: Wireless (LAN) medium access control (MAC) and physical layer (PHY) specifications," *ANSI/IEEE Std 802.11, 1999 Edition (R2003)*, 2003.

[27] C. E. Perkins, J. T. Malinen, R. Wakikawa, E. M. Belding-Royer, and Y. Sun, "IP address autoconfiguration for ad hoc networks." Internet Draft (work in progress) draft-perkins-manet-autoconf-01.txt, IETF, November 2001.

[28] N. H. Vaidya, "Weak duplicate address detection in mobile ad hoc networks," in *Proceedings of the 3rd Annual ACM International Symposium on Mobile Ad Hoc Networking and Computing (MobiHoc '02)*, pp. 206–216, June 2002. Lausanne, Switzerland.

[29] K. Weniger, "Passive duplicate address detection in mobile ad hoc networks," in *Proceedings of the Annual IEEE Wireless Communications and Networking Conference (WCNC '03)*, vol. 3, pp. 1504–1509, March 2003. New Orleans, LA, USA.

[30] Y. Sun and E. M. Belding-Royer, "A study of dynamic addressing techniques in mobile ad hoc networks," *Wireless Communications and Mobile Computing*, vol. 4, pp. 315–329, April 2004.

[31] K. Weniger, "PACMAN: Passive autoconfiguration for mobile ad-hoc networks," *IEEE Journal on Selected Areas in Communications*, vol. 23, pp. 507–519, March 2005.

[32] B. Wehbi, "Address autoconfiguration in ad hoc networks." Internal Report, Departement Logiciels Reseaux, Institute National des Telecommunications. Online: `http://www.bachwehbi.net/autoconf_report.pdf`, May 2005.

[33] K. Weniger and M. Zitterbart, "Address autoconfiguration in mobile ad hoc networks: Current approaches and future directions," *IEEE Network*, vol. 18, pp. 6–11, August 2004.

[34] L. Lamont, M. Wang, L. Villasenor, T. Randhawa, and S. Hardy, "Integrating WLANs and MANETs to the IPv6 based Internet," in *Proceedings of the 38th Annual IEEE International Conference on Communications (ICC '03)*, vol. 2, pp. 1090–1095, May 2003. Anchorage, AK, USA.

[35] C.-Y. Wang, C.-Y. Li, R.-H. Hwang, and Y.-S. Chen, "Global connectivity for mobile IPv6-based ad hoc networks," in *Proceedings of the 19th Annual IEEE International Conference on Advanced Information Networking and Applications (AINA '05)*, vol. 2, pp. 807–812, March 2005. Taipei, Taiwan.

[36] M. Günes and J. Reibel, "An IP address configuration algorithm for zeroconf mobile multihop ad hoc networks," in *Proceedings of the International Workshop on Broadband Wireless Ad Hoc Networks and Services*, September 2002. Sophia Antipolis, France.

[37] S. Nesargi and R. Prakash, "MANETconf: Configuration of hosts in a mobile ad hoc network," in *Proceedings of the 21st Annual IEEE Conference on Computer Communications (INFOCOM '02)*, vol. 2, pp. 1059–1068, June 2002. New York, NY, USA.

[38] M. Bagnulo, I. Soto, A. Garcia-Martinez, and A. Azcorra, "Random generation of interface identifiers." Internet Draft (work in progress) draft-soto-mobileip-randim-iids-00.txt, IETF, January 2002.

[39] K. S. King and N. Smith, "Dynamic addressing and mobility in tactical hybrid ad hoc networks," in *Proceedings of the 24th Annual IEEE Military Communications Conference (MILCOM '05)*, vol. 5, pp. 2930–2935, October 2005. Atlantic City, NJ, USA.

[40] H. Ammari and H. El-Rewini, "Integration of mobile ad hoc networks and the Internet using mobile gateways," in *Proceedings of the 18th Annual IEEE International Parallel and Distributed Processing Symposium (IPDPS '04)*, pp. 218–225, April 2004. Santa Fe, NM, USA.

[41] M. K. Denko and C. Wei, "An architecture for integrating mobile ad hoc networks with the Internet using multiple mobile gateways," in *Proceedings of the 18th Annual IEEE Canadian Conference on Electrical and Computer Engineering (CCECE '05)*, pp. 1097–1102, May 2005. Saskatchewan, Canada.

[42] Y. Mo, J. Huang, and B. Huang, "MANET node based mobile gateway with unspecific MANET routing protocol," in *Proceedings of the 6th Annual IEEE International Symposium on Communications and Information Technologies (ISCIT '06)*, pp. 886–889, October 2006. Bangkok, Thailand.

[43] D. B. Green, "Stryker brigade combat team IPv6 transition modeling and simulation study," in *Proceedings of the 24th Annual IEEE Military Communications Conference (MILCOM '05)*, vol. 4, pp. 2275–2281, October 2005. Atlantic City, NJ, USA.

[44] L. Kant, F. Anjum, and K. Young, "Design and analysis of scalable network centric warfare mechanisms," in *Proceedings of the 25th Army Science Conference (ASC '06)*, November 2006.

[45] C. Jelger, T. Noel, and A. Frey, "Gateway and address autoconfiguration for IPv6 ad hoc networks." Internet Draft (work in progress) draft-jelger-manet-gateway-autoconf-v6-02.txt, IETF, April 2004.

[46] A. Frey, "Autoconfiguration in IPv6 wireless ad hoc networks - stand alone daemon," October 2004. Online: `http://www-r2.u-strasbg.fr/~frey/safari/autoconf.html`, accessed August 23, 2008.

[47] C. Jelger, *Gestion des équipments mobiles et communications de group dans l'Internet Nouvelle Génération.* PhD thesis, Université Louis Pasteur, Strasbourg, France, October 2004. (in French).

[48] M. Chandra and A. Roy (eds.), "Extensions to ospf to support mobile ad hoc networking." Internet Draft (work in progress) draft-ietf-ospf-manet-or-00.txt, IETF, February 2008.

[49] R. Ogier and P. Spagnolo, "MANET extension of OSPF using CDS flooding." Internet Draft (work in progress) draft-ietf-ospf-manet-mdr-02.txt, IETF, June 2008.

[50] E. Bacelli, P. Jacquet, D. Nguyen, and T. Clausen, "OSPF MPR extension for ad hoc networks." Internet Draft (work in progress) draft-ietf-ospf-manet-mpr-01.txt, IETF, July 2008.

[51] J. Moy, "OSPF version 2," April 1998. Request for Comments 2328, IETF.

[52] R. Coltun, D. Ferguson, and J. Moy, "OSPF for IPv6," December 1999. Request for Comments 2740, IETF.

[53] R. Coltun, D. Ferguson, J. Moy, and A. Lindem (ed.), "OSPF for IPv6," July 2008. Request for Comments 5340, IETF.

[54] Z. J. Haas, "Panel report on ad hoc networks - MILCOM '97," *ACM SIGMOBILE Mobile Computing and Communications Review*, vol. 2, pp. 15–18, January 1998.

[55] T. R. Henderson, P. A. Spagnolo, and J. H. Kim, "A wireless interface type for OSPF," in *Proceedings of the 22nd Annual IEEE Military Communications Conference (MILCOM '03)*, vol. 2, pp. 1256–1261, October 2003. Boston, MA, USA.

[56] M. Chandra (ed.), "Extensions to OSPF to support mobile ad hoc networking." Internet Draft (work in progress) draft-chandra-ospf-manet-ext-03.txt, IETF, April 2005.

[57] R. Ogier and P. Spagnolo, "MANET extension of OSPF using CDS flooding." Internet Draft (work in progress) draft-ogier-manet-ospf-extension-04.txt, IETF, July 2005.

[58] T. R. Henderson, P. A. Spagnolo, and G. Pei, "Evaluation of OSPF MANET extensions," Tech. Rep. D950-10987-1, Boeing, July 2005. Online: `http://hipserver.mct.phantomworks.org/ietf/ospf`.

[59] J. T. Moy, *OSPF: Anatomy of an Internet Routing Protocol.* Reading, MA, USA: Addison-Wesley, 1998.

[60] J. T. Moy, *OSPF: Complete Implementation.* Reading, MA, USA: Addison-Wesley, 2001.

[61] J. Doyle and J. Carroll, *Routing TCP/IP*, vol. 1 of *CCIE Professional Development.* Indianapolis, IN, USA: Cisco Press, 2nd ed., 2006.

[62] P. A. Spagnolo and T. R. Henderson, "Comparison of proposed OSPF MANET extensions," in *Proceedings of the 25th Annual IEEE Military Communications Conference (MILCOM '06)*, October 2006. Washington, DC, USA.

[63] "Quagga software routing suite." Online: `http://www.quagga.net/`.

[64] R. Ogier and P. Spagnolo, "MANET extension of OSPF using CDS flooding." Internet Draft (work in progress) draft-ogier-manet-ospf-extension-06.txt, IETF, December 2005.

[65] "Wireshark: Network protocol analyzer." Online: `http://www.wireshark.org/`.

[66] C. Bettstetter, G. Resta, and P. Santi, "The node distribution of the random waypoint mobility model for wireless ad hoc networks," *IEEE Transactions on Mobile Computing*, vol. 2, pp. 257–269, July-September 2003.

[67] W. Ye, *Radio Propagation Models.* in *ns* Manual, Online: `http://www.isi.edu/~weiye/pub/propagation_ns.pdf`.

Appendix A. RTS/CTS Sequence Pseudocode

A.1 Event Compression

Procedure 1 Event-Compression RTS/CTS

```
upon node $s$ is IDLE and has frame to send to node $d$
    set $rts\_flag = false$
    set $cts\_flag = false$
    retrieve entire set of nodes, $L$
    for every node $i$ in $L$ such that $i \neq s$ do
        compute transmission attempt from $s$ to $i$
        if attempt == valid then
            if $i == d$ then
                set $rts\_flag = true$
            else
                NAV/backoff timer of $i$ adjusted
    if $rts\_flag == true$ then
        for every node $i$ in $L$ such that $i \neq d$ do
            compute transmission attempt from $d$ to $i$
            if attempt == valid then
                if $i == s$ then
                    set $cts\_flag = true$
                else
                    NAV/backoff timer of $i$ adjusted
    if $(rts\_flag == true)\&(cts\_flag == true)$ then
        proceed to original frame transmission
    else
        backoff and attempt later
```

A.2 Neighbor List

Procedure 2 Neighbor List RTS/CTS

```
upon node $s$ is IDLE and has frame to send to node $d$
    set $rts\_flag = false$
    set $cts\_flag = false$
    retrieve neighbor list, $nl_s$, of node $s$
    for every node $i$ in $nl_s$ such that $i \neq s$ do
        compute transmission attempt from $s$ to $i$
        if attempt == valid then
            if $i == d$ then
                set $rts\_flag = true$
            else
                NAV/backoff timer of $i$ adjusted
    if $rts\_flag == true$ then
        retrieve neighbor list, $nl_d$, of node $d$
        for every node $i$ in $nl_d$ such that $i \neq d$ do
            compute transmission attempt from $d$ to $i$
            if attempt == valid then
                if $i == s$ then
                    set $cts\_flag = true$
                else
                    NAV/backoff timer of $i$ adjusted
    if $(rts\_flag == true)\&(cts\_flag == true)$ then
        proceed to original frame transmission
    else
        backoff and attempt later
```

A.3 Simplified Neighbor List

Procedure 3 Simplified Neighbor List RTS/CTS

```
upon node $s$ is IDLE and has frame to send to node $d$
    set $rts\_flag = false$
    set $cts\_flag = false$
    retrieve neighbor list, $nl_s$, of node $s$
    for every node $i$ in $nl_s$ such that $i \neq s$ do
        if $i == d$ then
            compute transmission attempt from $s$ to $d$
            if attempt == valid then
                set $rts\_flag = true$
        else
            NAV/backoff timer of $i$ adjusted
    if $rts\_flag == true$ then
        retrieve neighbor list, $nl_d$, of node $d$
        for every node $i$ in $nl_d$ such that $i \neq d$ do
            if $i == s$ then
                compute transmission attempt from $d$ to $s$
                if attempt == valid then
                    set $cts\_flag = true$
            else
                NAV/backoff timer of $i$ adjusted
    if $(rts\_flag == true)\&(cts\_flag == true)$ then
        proceed to original frame transmission
    else
        backoff and attempt later
```